Title	STUDIES ON THE KINETICS AND MECHANISM OF THE REACTION OF DITHIOCARBAMATO-METAL COMPLEXES WITH HALOGENS AND THIURAM DISULFIDE
Author(s)	喜多, 英敏
Citation	大阪大学, 1979, 博士論文
Version Type	VoR
URL	https://hdl.handle.net/11094/2264
rights	
Note	

STUDIES ON THE KINETICS AND MECHANISM OF THE REACTION OF DITHIOCARBAMATO-METAL COMPLEXES WITH HALOGENS AND THIURAM DISULFIDE

（ジチオカーバマト金属錯体とハロゲンおよび
チウラムジスルフィドとの反応の速度論的研究）

1 9 7 9

HIDETOSHI KITA

Department of Applied Chemistry
Osaka University

PREFACE

This thesis was performed under the guidance by Professor Toshio Tanaka of the Department of Applied Chemistry, Faculty of Engineering, Osaka University.

The contents of this thesis are composed of the following papers.

(1) The Kinetics and Mechanisms of Reaction of Iodine with Bis(*N*,*N*-diethyldithiocarbamato)dimethyltin(IV) and Related Compounds.
H. Kita, K. Tanaka, and T. Tanaka,
Bull. Chem. Soc. Jpn., 48, 2816 (1975).

(2) Kinetics and Mechanism of the Reaction of Iodine with Bis(*N*,*N*-di-*n*-butyldithiocarbamato)zinc(II).
H. Kita, K. Tanaka, and T. Tanaka,
Inorg. Chim. Acta, 21, 229 (1977).

(3) Kinetics and Mechanism of the Oxidation of Bis(μ-dibutyldithiocarbamato-S,S')-digold(I) by Halogens.
H. Kita, K. Itoh, K. Tanaka, and T. Tanaka,
Bull. Chem. Soc. Jpn., 51, 3530 (1978).

(4) Kinetics and Mechanism of the Oxidation Reaction of Dithiocarbamato Copper(I) and Silver(I) Complexes with Thiuram Disulfide.
H. Kita, S. Miyake, K. Tanaka, and T. Tanaka,
to be published.

I would like to express my sincere thanks to Professor Toshio Tanaka for his invaluable guidance and constant encouragement throughout this work. I am also grateful to Dr. Koji Tanaka for his interest and encouragement from the

beginning of the work. Thanks are also due to Dr. Katsuhiko Kawakami, Dr. Gen-etsu Matsubayashi, and Dr. Masa-aki Haga for their helpful suggestions and discussions. The author is much indebted to Mr. Kazuyuki Itoh for assistance with the experiments in Chapter 3, and to Mr. Shin-ichi Miyake for help with measurements and calculations in Chapter 4. It is a pleasure to express my gratitude to all the members of Tanaka laboratory for their friendship. Last but not least, I wish to thank my parents for their understanding and encouragement.

Hidetoshi Kita
Hidetoshi Kita

Suita, Osaka
December, 1978

CONTENTS

Chapter 4 The Reaction of the Dithiocarbamates of Copper(I) and Silver(I) with Thiuram Disulfide

GENERAL INTRODUCTION

The wide industrial importance of dithiocarbamates and their derivatives as metal complexing agents, herbicides, fungicides, vulcanization accelerators etc. has resulted in considerable research.[1-4) Especially, it has been established during the past decade that metal complexes with dithiocarbamate ligands (1) exhibit many unusual properties such as spin

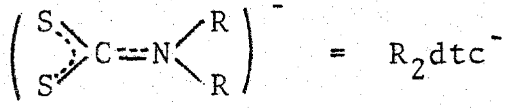

1

isomerism of the iron(III) complexes[5) and oligomeric structures of the copper(I) (tetrameric),[6) silver(I) (hexameric),[7) and gold(I) (dimeric)[8) complexes.

Quite recently, the dithiocarbamate ligand has been shown to possess the ability to stabilize metal ions in unusually high formal oxidation states. This ability has been rationalized in terms of delocalization of electronic charges[9) and S-S interligand interactions,[10) as shown in the canonical structures of b and c, respectively. This interesting property

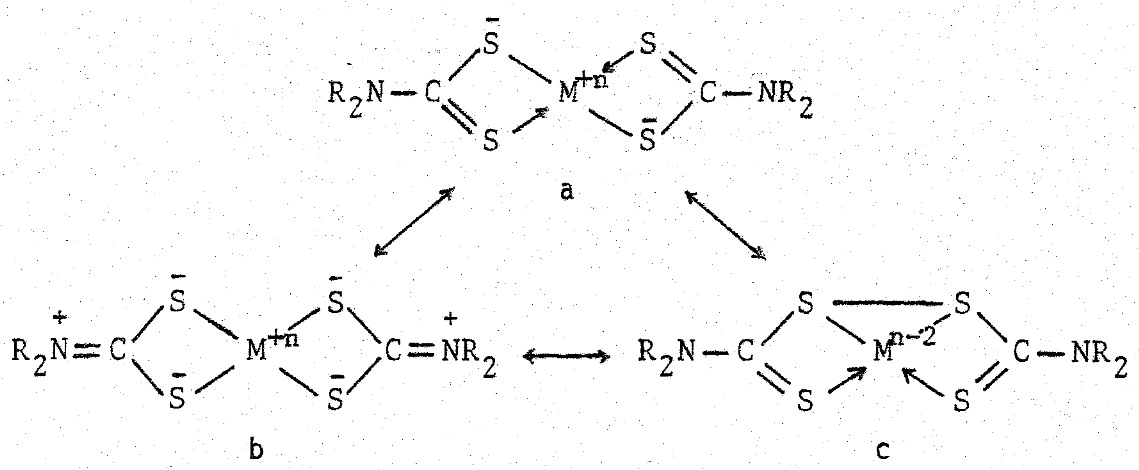

seems to facilitate a number of studies[11] on the reaction of dithiocarbamato metal complexes with oxidizing agents such as halogens, boron trifluoride etc. All the works in this field, however, has been of a preparative nature and there has been no mechanistic study. Thus, the author has initiated a detailed kinetic study in order to expand the knowledge in this area.

The purpose of this thesis is to elucidate the mechanism of oxidation reactions of dithiocarbamato metal complexes with halogens and thiuram disulfide.

This thesis consists of four chapters. Chapter 1 and 2 describe the reactions of iodine with diethyldithiocarbamato tin(IV) and dibutyldithiocarbamato zinc(II), respectively. In Chapter 3, the reactions of dibutyldithiocarbamato gold(I) dimer with iodine, bromine, and iodine bromide are discussed. The last chapter deals with the reactions of dithiocarbamate complexes of copper(I) and silver(I) with thiuram disulfide. The kinetics of these reactions were all investigated employing a stopped-flow technique.

References

1) G. D. Thorn and R. A. Ludwig, "The Dithiocarbamates and Related Compounds," Elsevier, Amsterdam, 1962.

2) D. Coucouvanis, *Prog. Inorg. Chem.,* 11, 233 (1970).

3) R. Eisenberg, *Prog. Inorg. Chem.,* 12, 295 (1970).

4) L. H. Pignolet, *Topics in Current Chemistry,* 56,91 (1975).

5) R. L. Martin and A. H. White, *Transition Met. Chem.,* 4, 113 (1968).

6) R. Hesse, *Arkiv Kemi,* 20, 481 (1963).

7) R. Hesse and L. Nilson, *Acta Chem. Scand.*, 23, 825 (1969); H. Yamaguchi, A. Kida, T. Uechi, and K. Yasukouchi, *Bull. Chem. Soc. Jpn.*, 49, 1271 (1976).

8) R. Hesse and P. Jennische, *Acta Chem. Scand.*, 26, 3855 (1972).

9) B. L. Edgar, D. J. Duffy, M. C. Palazzotto, and L. H. Pignolet, *J. Am. Chem. Soc.*, 95, 1125 (1973).

10) J. P. Fackler, Jr., *Prog. Inorg. Chem.*, 21, 55 (1976).

11) J. Willemse, J. A. Cras, J. J. Steggerda, and C. P. Keijzers, *Structure and Bonding*, 28, 83 (1976).

CHAPTER 1 REACTIONS OF IODINE WITH BIS(DIETHYLDITHIOCARBAMATO)DIMETHYLTIN(IV) AND RELATED COMPOUNDS

1-1 Introduction

A number of reactions of dithiocarbamato metal complexes with halogens have been studied.1-32) They are classified into the following two types; (i) the oxidation of the dithiocarbamato ligand by halogen into thiuram disulfide (1), R_4tds, or dipositive trithiolane (2), $[R_4\mathrm{bitt}]^{2+}$, which is an oxidation product of 1 by halogen, and (ii) the oxidation of the central metal of dithiocarbamato complexes by halogen. A short resume from the literature of such reactions is given in Table 1. The kinetics of these reactions, however, have been little studied.

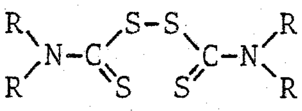

1

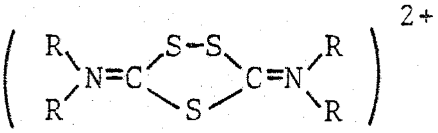

2

Recently, it has been noticed that $Me_2Sn(Et_2dtc)_2$ and $Me_2SnI(Et_2dtc)$ rapidly react with I_2 to give $Me_2SnI(Et_2dtc)$ and Me_2SnI_2 respectively, together with tetraethylthiuram disulfide. This chapter describes the kinetic and mechanistic study of these reactions in cyclohexane by the stopped-flow method. The stability constant of the charge-transfer complex between tetraethylthiuram disulfide and iodine is also reported.

Table 1 Oxidation products of the reactions of dithiocarbamato metal complexes with halogens.

(i) Oxidation of dithiocarbamato ligand into thiuram disulfide (tds) or dipositive trithiolane (bitt)

Reactant	Product	Ref.
$M(dtc)_2$ (M=Zn, Cd, Hg)	$MX_2(tds)$ (X=Cl, Br, I)	4, 10
$[Zn(dtc)_3]^-$	$[ZnI_2(dtc)]^-$, tds	17
$Pb(dtc)_2$	$PbX(dtc)$, tds (X=Br, I)	7
$M(dtc)_3$ (M=As, Sb, Bi)	$MX(dtc)_2$, tds (X=Br, I)	18, 25
$Me_2Sn(dtc)_2$	$Me_2SnI(dtc)$, Me_2SnI_2, tds	19
$Fe(dtc)_3$	$FeX(dtc)_2$, tds (X=I, I_3)	26
$PR_3Pt(dtc)_2$	$PR_3PtI(dtc)$, tds	28
tds	[bitt]2X (X=Cl, Br, I_3)	29, 30
$HgI_2(tds)$	$[bitt][Hg_2I_6]$	31, 32
$Cu(dtc)_2$, $Fe(dtc)_3$, $FeCl(dtc)_2$	[bitt]X (X=$CuBr_4^{2-}$, $2FeCl_4^-$)	5, 32

(ii) Oxidation of the central metal

Reactant	Product	Ref.
$[Cu(dtc)]_4$	$CuX_2(dtc)$ (X=Cl, Br)	3, 4, 6
$[Cu(dtc)]_4$, $Cu(dtc)_2$	$[Cu(dtc)_2]I_3$	9, 12
$[Au(dtc)]_2$	$[Au(dtc)_2][AuX_2]$, $AuX_2(dtc)$ (X=Cl, Br, I)	1, 2
$Ni(dtc)_2$	$[Ni(dtc)_3]X$ (X=Cl, Br, I_3)	4, 8, 9, 13
	$Ni(dtc)_2Br_2$	6
	$NiI(dtc)_2$	11
$M(dtc)_2$ (M=Pt, Pd)	$MX_2(dtc)_2$ (X=Br, I)	15
$Fe(dtc)_3$	$[Fe(dtc)_3]I_3$	26
$Ru(dtc)_3$	$RuI(dtc)_3 \cdot I_2$	27
$Mo(dtc)_4$	$[Mo(dtc)_4]X$ (X=Br, I, I_3)	14, 16, 21, 24
$OMo(dtc)_2$	$OMoX_2(dtc)_2$ (X=Cl, Br)	20, 23
$Cp_2V(dtc)$	$[Cp_2V(dtc)]I_3$	22

1-2 Experimental

Materials. Bis(diethyldithiocarbamato)dimethyltin(IV), $\mathrm{Me_2Sn(Et_2dtc)_2}$ (dtc= $\mathrm{S_2CN}{<}$), was obtained as has been described in the literature.$^{33)}$ Diethyldithiocarbamatodimethyliodotin(IV), $\mathrm{Me_2SnI(Et_2dtc)}$, was prepared by the reaction of $\mathrm{Me_2SnCl(Et_2dtc)}$ with a large excess of NaI in acetone in the manner described previously$^{33)}$; it was then recrystallized from ligroin; mp 124°C. Anal. Found: C, 19.82; H, 4.04; N, 3.50%. Calcd for $\mathrm{C_7H_{16}NS_2ISn}$: C, 19.84; H, 3.81; N, 3.31%.

Iodine was purified by sublimation five times. Commercially available tetraethylthiuram disulfide, $\mathrm{Et_4tds}$ (tds= ${>}\mathrm{NC(S)S_2C(S)N}{<}$), was recrystallized from ligroin; mp 70°C. Cyclohexane used as a solvent in the kinetic experiments was purified in the usual manner.$^{34)}$

Reactions. (i) A solution of $\mathrm{I_2}$ (1.02 mmol) in benzene (20 ml) was added to $\mathrm{Me_2Sn(Et_2dtc)_2}$ (2.38 mmol) in the same solvent (20 ml) at room temperature. The solution was stirred for 30 min, and then evaporated to dryness under reduced pressure. The resulting solid was recrystallized from ligroin to afford white crystals of $\mathrm{Me_2SnI(Et_2dtc)}$ (1.87 mmol). The filtrate after recrystallization was evaporated to dryness again to give $\mathrm{Et_4tds}$ (0.84 mmol).

(ii) A benzene solution (20 ml) containing $\mathrm{I_2}$ (0.5 mmol) and $\mathrm{Me_2SnI(Et_2dtc)}$ (1.9 mmol) was stirred for 1 hr at room temperature; the subsequent application of the procedure described above gave $\mathrm{Me_2SnI_2}$ (0.6 mmol).

(iii) A benzene solution (20 ml) of $\mathrm{Me_2Sn(Et_2dtc)_2}$ (2.3 mmol) was added to the excess of $\mathrm{I_2}$ (4.5 mmol) in the same solvent

(20 ml) at room temperature. The solution was then stirred for 3.5 hr, filtered, and evaporated to a small volume. The precipitate which appeared was collected by filtration and recrystallized from petroleum ether to afford $Me_2SnI(Et_2dtc)$ (0.3 mmol). The filtrate was evaporated to give a solid product, from which Me_2SnI_2 (1.5 mmol) was obtained.

Spectra. The electronic spectra were recorded on a Hitachi 124 spectrophotometer. The infrared spectra were measured in Nujol mulls on a Hitachi EPI-L spectrophotometer. Rapid scanning spectra were measured with a Union RA-1300 stopped-flow rapid scan analyzer.

Kinetics. Kinetic experiments were carried out under pseudo-first-order conditions at 25°C, using at least a tenfold excess amount of either iodine or the tin compound. The rate of reaction was followed by monitoring the transmittance at a fixed wavelength in the electronic spectra of the reaction mixture, using a Union RA-102 stopped-flow spectrophotometer equipped with a 1.0 cm quartz cell. The instrument was thermostated to ±0.2°C. The transmittance change with time was monitored on a Hitachi V-108 memoriscope. Transmittance-time data were obtained by photographing the scope. For each run at least four measurements were carried out. Plots of $\ln(A_\infty - A_t)$ vs. time showed a good linearity for at least 3 half-lives and from the slopes pseudo-first-order rate constants, k_{obsd}, were evaluated by the least-squares method, where A_t and A_∞ are absorbances at a given wavelength at a time t and the end of the reaction, respectively.

1-3 Results and Discussion

Stoichiometry of the Reaction. The reaction of I_2 with excess $Me_2Sn(Et_2dtc)_2$ rapidly proceeds to give $Me_2SnI(Et_2dtc)$ and Et_4tds in good yields. Iodine also reacts with $Me_2SnI(Et_2dtc)$ to afford Me_2SnI_2 and Et_4tds; this reaction is reversible. The forward and backward reactions require a few minutes and several days respectively to come to an equilibrium. Thus, the stoichiometry for the reaction of $Me_2Sn(Et_2dtc)_2$ with I_2 may be expressed as follows:

$$Me_2Sn(Et_2dtc)_2 + \frac{1}{2}I_2 \xrightarrow{\text{fast}} Me_2SnI(Et_2dtc) + \frac{1}{2}Et_4tds \qquad (1)$$

$$Me_2SnI(Et_2dtc) + \frac{1}{2}I_2 \underset{\text{very slow}}{\overset{\text{slow}}{\rightleftharpoons}} Me_2SnI_2 + \frac{1}{2}Et_4tds \qquad (2)$$

Stability Constant of the Charge-transfer Complex between I_2 and Et_4tds. By analogy with the formation of a stable charge-transfer complex between I_2 and *N*-methylthioacetoamide,[35)] *N*-methylthiocarbamate[35)] or other sulfur containing compounds,[35, 36)] I_2 may be expected to form a complex with Et_4tds, which is the reaction product between I_2 and $Me_2Sn(Et_2dtc)_2$ or $Me_2SnI(Et_2dtc)$. In accordance with this, cyclohexane solutions containing Et_4tds and I_2 exhibit an absorption at 355 nm, which is intensified with an increase in the amounts of I_2, as is shown in Figure 1. Thus, the 355 nm band can unequivocally be assigned to the CT transition from Et_4tds to I_2. Figure 2 shows the electronic spectra of I_2 in cyclohexane containing varying amounts of Et_4tds. The 520 nm band due to I_2 is shifted to a short wavelength (470 nm) by adding Et_4tds, and an isosbestic point is observed at 515 nm. The continuous-variation method at 470 nm

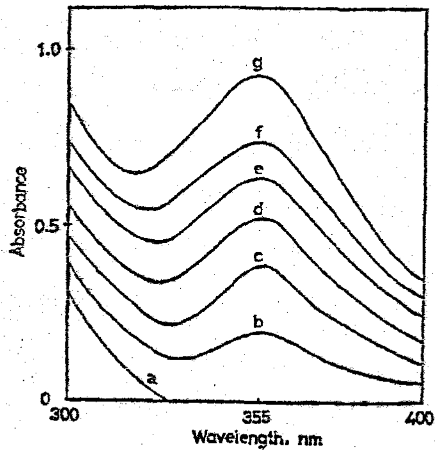

Fig. 1. Absorption spectra of Et_4tds in cyclohexane (1.0×10^{-4} M) containing varying amounts of I_2: (a) 0, (b) 1.0×10^{-3}, (c) 2.0×10^{-3}, (d) 3.0×10^{-3}, (e) 4.0×10^{-3}, (f) 5.0×10^{-3}, (g) 8.0×10^{-3} M (25 °C).

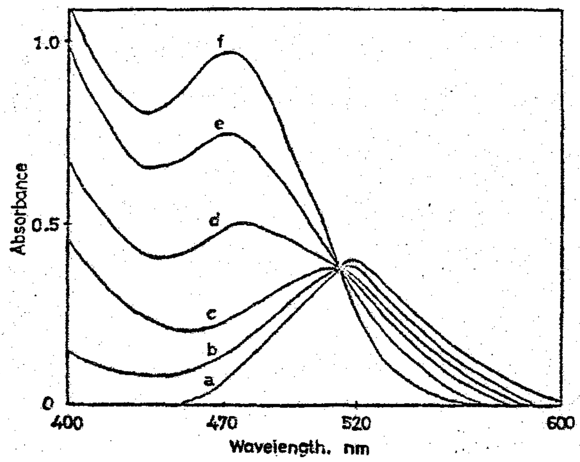

Fig. 2. Absorption spectra of I_2 in cyclohexane (8.0×10^{-4} M) containing varying amounts of Et_4tds: (a) 0, (b) 8.0×10^{-4}, (c) 1.6×10^{-3}, (d) 4.0×10^{-3}, (e) 8.0×10^{-3}, (f) 1.6×10^{-2} M (25 °C).

revealed that the composition of the CT complex is 1:1. Thus, the following equilibrium takes place in solution:

$$I_2 + Et_4tds \xrightleftharpoons{K} I_2\cdot Et_4tds \qquad (3)$$

The equilibrium constant, as calculated from the absorbances at 470 nm ($\varepsilon_{max} = 2.14 \times 10^3$) by means of the Rose-Drago equation,[37)] was $K = 3.75(\pm0.01) \times 10^2$ in cyclohexane at 25°C.

Reaction of I_2 with Excess $Me_2Sn(Et_2dtc)_2$ or $Me_2SnI(Et_2dtc)$. The rapid scanning spectra for the reaction of I_2 with excess $Me_2Sn(Et_2dtc)_2$ are depicted in Figure 3, which reveals

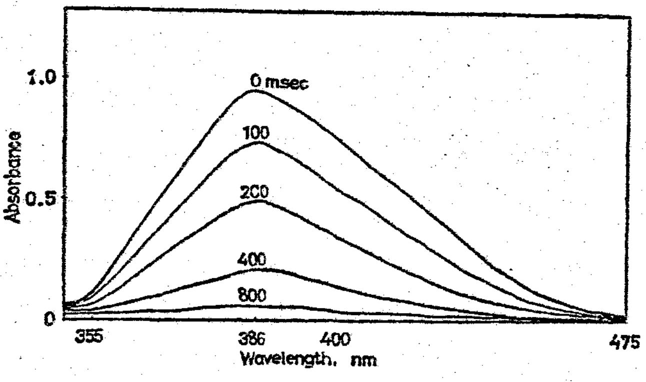

Fig. 3. The decay of the electronic spectrum after mixing I_2 (1.7×10^{-3} M) with $Me_2Sn(dtc)_2$ (3.0×10^{-2} M) in cyclohexane at 25 °C.

that a strong band appears at 386 nm immediately after mixing and that the band decays with a half-life of about 200 ms. An almost identical half-life of decay was found at the 520 nm band. The reaction of I_2 with excess $Me_2SnI(Et_2dtc)$ also showed the decay of the 386 nm band with a half-life of about 40 s. However, the CT band due to $I_2 \cdot Et_4tds$ at 355 nm was not observed at all.

The rate of reaction was followed by measuring the transmittances at 386 and 520 nm of a solution right after the mixing of I_2 with excess $Me_2Sn(Et_2dtc)_2$. Plots of $\ln(A_t - A_\infty)$ vs. time showed a good linearity. Thus, the reaction apparently obeys the first-order kinetics with respect to I_2. Observed pseudo-first-order rate constants, k_{obsd}, obtained at various concentrations of $Me_2Sn(Et_2dtc)_2$ are collected in Table 2.

Table 2 Observed rate constants for the reaction of I_2 with excess $Me_2Sn(Et_2dtc)_2$ in cyclohexane at 25°C.

$[Me_2Sn(Et_2dtc)_2]$ / M	$[I_2]$ / M	k_{obsd} / s^{-1}	
		386 nm	520 nm
3.00×10^{-3}	3.00×10^{-4}	0.263	0.268
6.00×10^{-3}		0.527	0.555
9.00×10^{-3}		0.846	0.761
1.20×10^{-2}		1.08	1.02
1.50×10^{-2}		1.32	1.32
1.80×10^{-2}		1.57	1.63
2.40×10^{-2}		2.24	2.16

Plots of the rate constants obtained from the decay of the transmittances at 386 and 520 nm against the concentration of $Me_2Sn(Et_2dtc)_2$ showed a good linearity, as may be seen in

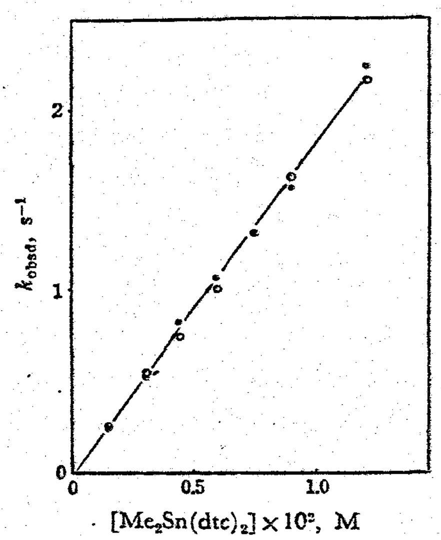

Fig. 4. Plots of the apparent rate constant against the $Me_2Sn(dtc)_2$ concentrations; ● 386 nm, ○ 520 nm.

Figure 4; this indicates that the reaction is first-order in both I_2 and $Me_2Sn(Et_2dtc)_2$.

Taking into account this result and the fact that I_2 can form CT complexes with various sulfur-containing compounds,35, 36) the band at 386 nm may be assigned to the CT complex formed between I_2 and $Me_2Sn(Et_2dtc)_2$ in the initial process. The addition of Et_4tds to the reactant solution caused no appreciable decrease in the rate of reaction. Thus, the following pathways for the reaction may reasonably be suggested:

$$Me_2Sn(Et_2dtc)_2 + I_2 \overset{K_1}{\rightleftharpoons} Me_2Sn(Et_2dtc)_2 \cdot I_2 \qquad (4)$$

$$Me_2Sn(Et_2dtc)_2 \cdot I_2 \xrightarrow{k_1} Me_2SnI(Et_2dtc) + [I\text{-}Et_2dtc] \qquad (5)$$

$$[I\text{-}Et_2dtc] + Me_2Sn(Et_2dtc)_2 \xrightarrow{fast} Me_2SnI(Et_2dtc) + Et_4tds \qquad (6)$$

Reaction (5) represents the rate-determining step, producing unstable $[I\text{-}Et_2dtc]$. Although there is no evidence for the formation of $[I\text{-}Et_2dtc]$ as an intermediate, a somewhat analogous species, ISCN, has been reported to exist in the following equilibrium:38)

$$I^- + (SCN)_2 \rightleftharpoons I(SCN)_2^- \rightleftharpoons ISCN + SCN^- \qquad (7)$$

It may be possible that the two molecules of [I-Et_2dtc] produced in Eq. (5) react with each other to afford I_2 and Et_4tds, but this reaction seems not to occur, since no band was observed at 355 nm (due to $I_2 \cdot Et_4$tds) at all in the presence of excess $Me_2Sn(Et_2dtc)_2$. Instead, [I-Et_2dtc] must react rapidly with excess $Me_2Sn(Et_2dtc)_2$ to give $Me_2SnI(Et_2dtc)$ and Et_4tds, as is shown in Eq. (6). According to this reaction scheme, k_{obsd} can be expressed by Eq. (8):

$$k^{(1)}_{obsd} = \frac{K_1k_1[Me_2Sn(Et_2dtc)_2]}{1 + K_1[Me_2Sn(Et_2dtc)_2]} \qquad (8)$$

If $K_1[Me_2Sn(Et_2dtc)_2]$ is negligibly small compared with unity, $k^{(1)}_{obsd}$ is reduced to $K_1k_1[Me_2Sn(Et_2dtc)_2]$. This expression is consistent with the plots of k_{obsd} against the concentration of $Me_2Sn(Et_2dtc)_2$ with a zero intercept (Figure. 4). Thus, K_1k_1 is obtained as 1.84×10^2 $M^{-1}s^{-1}$.

Kinetic experiments on the reaction of $Me_2SnI(Et_2dtc)$ with I_2 were carried out by monitoring the transmittance only at 386 nm, since there was no marked change in the transmittance at 520 nm in this system because of the low solubility of $Me_2SnI(Et_2dtc)$ in cyclohexane. The k_{obsd} values obtained at various concentrations of $Me_2SnI(Et_2dtc)$ are listed in Table 3, which shows the reaction to be first-order in both $Me_2SnI(Et_2dtc)$ and I_2.

Table 3 Observed rate constants for the reaction of I_2 with excess $Me_2SnI(Et_2dtc)$ in cyclohexane at 25°C.

$[Me_2SnI(Et_2dtc)]$ M	$[I_2]$ M	k_{obsd} s^{-1}
7.59×10^{-3}	3.30×10^{-4}	1.10×10^{-2}
9.24×10^{-3}		1.24×10^{-2}
1.25×10^{-2}		1.59×10^{-2}
1.55×10^{-2}		2.08×10^{-2}

By analogy with the $Me_2Sn(Et_2dtc)_2$-I_2 system, the following pathways may be postulated, where $K_2k_2 = 1.37\ M^{-1}s^{-1}$:

$$Me_2SnI(Et_2dtc) + I_2 \overset{K_2}{\rightleftarrows} Me_2SnI(Et_2dtc)\cdot I_2 \qquad (9)$$

$$Me_2SnI(Et_2dtc)\cdot I_2 \xrightarrow{k_2} Me_2SnI_2 + [I\text{-}Et_2dtc] \qquad (10)$$

$$[I\text{-}Et_2dtc] + Me_2SnI(Et_2dtc) \xrightarrow{fast} Me_2SnI_2 + Et_4tds \qquad (11)$$

Since both K_1 and K_2 are unknown, K_1k_1 and K_2k_2 have been difficult to analyze quantitatively.

Reaction of $Me_2Sn(Et_2dtc)_2$ with excess I_2. The rate of reaction was determined from the decay of the transmittance at 386 nm. A good linear relationship between the $\ln(A_t - A_\infty)$* and the time was observed, except for the final short period, in which the 355 nm band arising from the product of $I_2\cdot Et_4tds$ is intensified and the tail of this band is overlapped with the 386 nm band. The k_{obsd} values obtained at various concentrations of I_2 are listed in Table 4. Plots of k_{obsd} vs. the square of I_2 concentrations gave a straight line in the presence of a large

---

* Here, A_∞ was assumed to be zero.

Table 4 Observed rate constants for the reaction of $Me_2Sn(Et_2dtc)_2$ with excess I_2 in cyclohexane at 25°C.

$[Me_2Sn(Et_2dtc)_2]$ / M	$[I_2]$ / M	k_{obsd} / s^{-1}
5.10×10^{-5}	5.02×10^{-4}	8.20×10^{-2}
	1.05×10^{-3}	4.36×10^{-2}
	1.50×10^{-3}	4.20×10^{-2}
	2.10×10^{-3}	6.08×10^{-2}
	2.51×10^{-3}	8.77×10^{-2}
	3.01×10^{-3}	1.13×10^{-1}

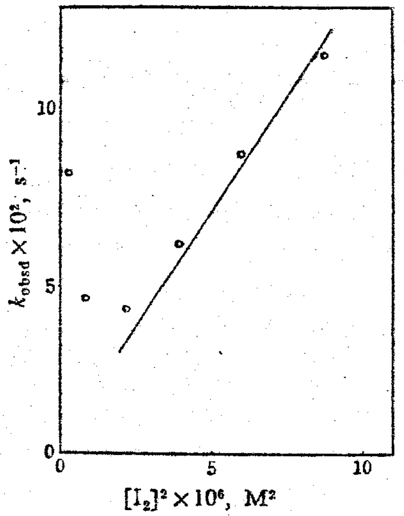

Fig. 5. Plots of the apparent rate constant against the square of the I_2 concentrations; $Me_2Sn(dtc)_2$ 5.1×10^{-5} M.

excess of I_2, while a significant deviation from it was observed in the presence of a small excess of I_2, as is shown in Figure 5. These results may be interpreted by assuming the following reaction pathways shown in Scheme.

One of the pathways involves the formation of the 1:2 adduct between $Me_2Sn(Et_2dtc)_2$ and I_2, which undergoes either consecutive (k_4 and k_2 in Scheme) or simultaneous (k_3) degradation to yield

Scheme

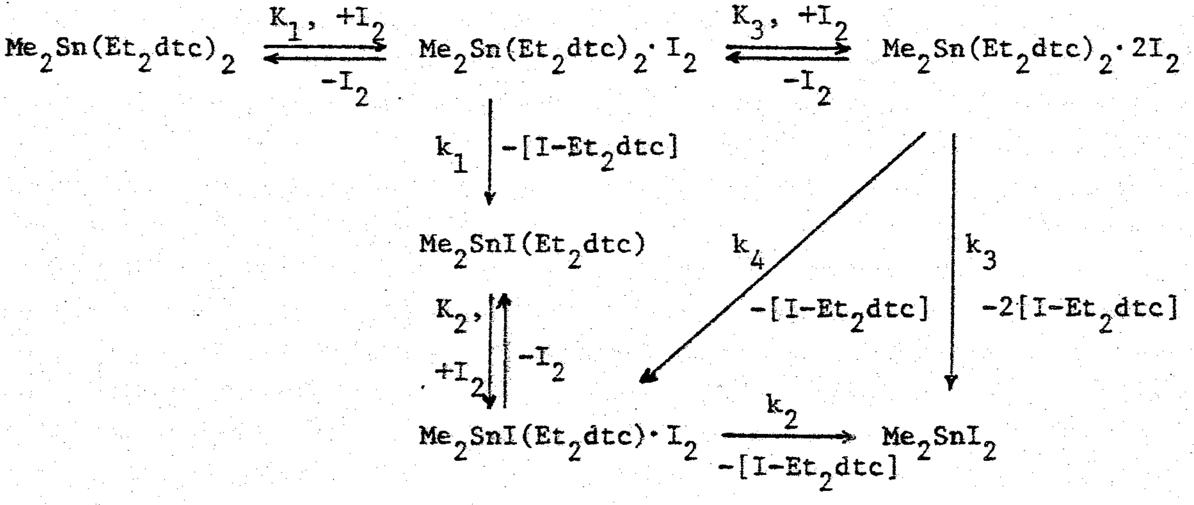

Me_2SnI_2 and $I_2 \cdot Et_4tds$. These processes can well explain the second-order dependence of the I_2 concentration. Taking into account the result that the reaction is much faster than that of I_2 with excess $Me_2SnI(Et_2dtc)$, the simultaneous degradation of the 1:2 adduct is preferable to the consecutive one. Another route is the successive formation of two 1:1 adducts, $Me_2Sn(Et_2dtc)_2 \cdot I_2$ and $Me_2SnI(Et_2dtc) \cdot I_2$, followed by degradation such as has been described above. This pathway leads us to the assumption that the reaction obeys the first-order kinetics in the I_2 concentration, because $K_1k_1 \gg K_2k_2$. It may, therefore, be assumed that, in the presence of a small excess of I_2, the processes *via* both the 1:1 and 1:2 adducts take place. Thus, in the presence of a large excess of I_2, the rate constant can be expressed by Eq. (12):

$$k_{obsd}^{(2)} = \frac{K_1K_3k_3[I_2]^2}{1 + K_1K_3[I_2]^2} \qquad (12)$$

If $K_1K_3[I_2]^2$ is negligibly small compared with unity, one can obtain $k_{obsd}^{(2)} = K_1K_3k_3[I_2]^2$, which conincides with the experimental data, and $K_1K_3k_3 = 1.34 \times 10^4\ M^{-2}s^{-1}$.

There are two possible mechanisms to form the unstable 1:2 adduct between $Me_2Sn(Et_2dtc)_2$ and I_2. One is a nucleophilic attack of two I_2 molecules on the tin atom. This is, however, not likely to occur, since no eight-coordination of tin is common. The other mechanism is an electrophilic attack of I_2 on the sulfur of separate dithiocarbamato ligands in a given complex, such as is shown in 3.

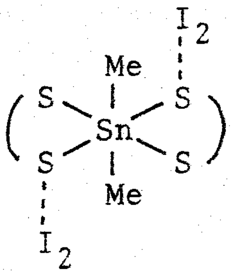

3: $S^\frown S = S_2CNEt_2$

This can be assumed on the basis of the fact that I_2 forms CT complexes with various sulfur-containing compounds.35, 36)

In conclusion, we propose that the reaction proceeds through a transition state involving a six-membered ring formed by the electrophilic attack of I_2 on the sulfur as follows:

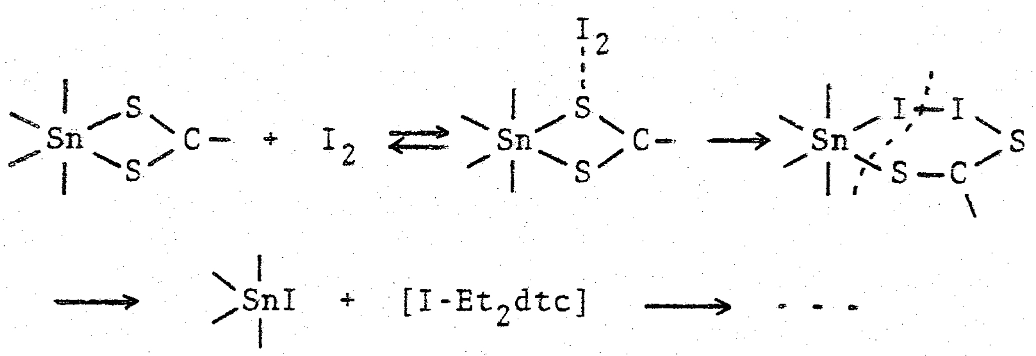

This mechanism predicts that the stronger Sn-S bond would be the less reactive toward I_2. This is consistent with the present result that the rate of reaction of $Me_2SnI(Et_2dtc)$ with

I_2 is slower than that of $Me_2Sn(Et_2dtc)_2$, since the ν(Sn-S) frequency of $Me_2SnI(Et_2dtc)$ (393 cm^{-1}) is fairly higher than that of $Me_2Sn(Et_2dtc)_2$ (366 cm^{-1}).

1-4 Summary

The reactions of $Me_2SnL(Et_2dtc)$ (L= Et_2dtc and I) with I_2 in cyclohexane were investigated employing a stopped-flow technique at 25°C. The kinetic data indicate that the reaction in the presence of a large excess of $Me_2SnL(Et_2dtc)$ proceeds *via* a charge-transfer complex of $Me_2SnL(Et_2dtc)\cdot I_2$, which decomposes in the rate-determining step to yield $Me_2SnI(L)$ and unstable [I-Et_2dtc]. This unstable intermediate reacts with excess $Me_2SnL(Et_2dtc)$ to afford $Me_2SnI(L)$ and tetraethylthiuram disulfide. The reaction of $Me_2Sn(Et_2dtc)_2$ with a large excess of I_2 was also kinetically studied to reveal the formation of the 1:2 complex, $Me_2Sn(Et_2dtc)_2\cdot 2I_2$, as an intermediate; this intermediate then undergoes a simultaneous degradation to afford Me_2SnI_2 and tetraethylthiuram disulfide. The transition state in the reaction was discussed.

1-5 References

1) H. J. A. Blaauw, R. J. F. Nivard, and G. J. M. van der Kerk, *J. Organomet. Chem.*, 2, 236 (1964).

2) P. T. Beurskens, H. J. A. Blaauw, J. A. Cras, and J. J. Steggerda, *Inorg. Chem.*, 7, 805 (1968).

3) P. T. Beurskens, J. A. Cras, and J. J. Steggerda, *Inorg. Chem.*, 7, 810 (1968).

4) H. C. Brinkhoff, J. A. Cras, J. J. Steggerda, and J. Willemse, *Recl. Trav. Chim. Pays-Bas*, 88, 633 (1969).

5) J. Willemse, and J. J. Steggerda, *Chem. Comm.*, 1969 , 1123.

6) Y. Nigo, I. Masuda, and K. Shinra, *Chem. Comm.*, 1970, 476.

7) F. Bonati and G. Minghetti, *Chim. Ind. (Milan)*, 52 , 1204 (1970); *Chem. Abst.*, 74, 150581g (1971).

8) A. Avdeef, J. P. Fackler, Jr., and R. G. Fischer, Jr., *J. Am. Chem. Soc.*, 92, 6972 (1970).

9) H. C. Brinkhoff, *Recl. Trav. Chim. Pays-Bas*, 90, 377 (1971).

10) P. T. Beurskens, J. A. Cras, J. H. Noordik, and A. M. Spruijt, *J. Cryst. Mol. Struct.*, 1, 93 (1971).

11) J. Willemse, P. H. F. M. Rouwette, and J. A. Cras, *Inorg. Nucl. Chem. Lett.*, 8, 389 (1972).

12) J. G. Wijnhoven, T. E. M. van den Hark, and P. T. Beurskens, *J. Cryst. Mol. Struct.*, 2, 189 (1972).

13) J. P. Fackler, Jr., A. Avdeef, and R. G. Fischer, Jr., *J. Am. Chem. Soc.*, 95, 774 (1973).

14) A. Nieuwpoort, J. H. E. Moonen, and J. A. Cras, *Recl. Trav. Chim. Pays-Bas*, 92, 1086 (1973).

15) J. Willemse, J. A. Cras, J. G. Wijnhoven, and P. T. Beurskens, *Recl. Trav. Chim. Pays-Bas*, 92, 1199 (1973).

16) J. F. Rowbottom and G. Wilkinson, *Inorg. Nucl. Chem. Lett.*, 9, 675 (1973).

17) J. A. McCleverty and N. J. Morrison, *Chem. Comm.*, 1974, 1048.

18) G. E. Manoussakis, C. A. Tsipis, and C. C. Hadjikostas, *Can. J. Chem.*, 53, 1530 (1975).

19) H. Kita, K. Tanaka, and T. Tanaka, *Bull. Chem. Soc. Jpn.*, 48, 2816 (1975).

20) W. E. Newton, D. C. Bravard, and J. W. McDonald, *Inorg. Nucl. Chem. Lett.*, 11, 553 (1975).

21) A. Nieuwpoort, H. M. Claessen, and J. G. M. van der Linden, *Inorg. Nucl. Chem. Lett.*, 11, 869 (1975).

22) G. Fachinetti, S. D. Nero, and C. Floriani, *J. Chem. Soc., Dalton Trans.*, 1976, 203.

23) J. Dirand, L. Richard, and R. Weiss, *J. Chem. Soc., Dalton Trans.*, 1976, 278.

24) A. Nieuwpoort and J. J. Steggerda, *Recl. Trav. Chim. Pays-Bas*, 95, 250 (1976).

25) C. A. Tsipis and G. E. Manoussakis, *Inorg. Chim. Acta*, 18, 35 (1976).

26) E. A. Pasek and D. K. Straub, *Inorg. Chim. Acta*, 21, 23 (1977).

27) B. M. Mattson and L. H. Pignolet, *Inorg. Chem.*, 16, 488 (1977).

28) G. A. Katsoulos, G. E. Manoussakis, and C. A. Tsipis, *Inorg. Chim. Acta*, 30, L295 (1978).

29) H. H. Carbacho and L. L. Victoriano, *J. Inorg. Nucl. Chem.*, 37, 1327 (1975).

30) E. W. Ainscough and A. M. Brodie, *J. Chem. Soc., Dalton Trans.*, 1977, 565.

31) P. T. Beurskens, W. P. J. H. Bosman, and J. A. Cras, *J. Cryst. Mol. Struct.*, 2, 183 (1972).

32) J. Willemse, J. A. Cras, and P. J. H. A. M. van de Leemput, *Inorg. Nucl. Chem. Lett.*, 12, 255 (1976).

33) M. Honda, M. Komura, Y. Kawasaki, T. Tanaka, and R. Okawara, *J. Inorg. Nucl. Chem.*, 30, 3231 (1968).

34) J. A. Riddick and E. E. Toops, Jr., "Technique of Organic Chemistry," Vol. 7, 2nd ed., ed. by A. Weissberger, Interscience, New York, N. Y. (1955), p. 307.

35) K. R. Bhaskar, S. N. Bhat, A. S. N. Murthy, and C. N. R. Rao, *Trans. Faraday Soc.*, 62, 788 (1966).

36) G. Reichenbach, S. Santini, and U. Mazzucato, *J. Chem. Soc., Faraday Trans. 1*, 69, 143 (1973).

37) N. J. Rose and R. S. Drago, *J. Am. Chem. Soc.*, 81, 6138 (1959).

38) C. Long and D. A. Skoog, *Inorg. Chem.*, 5, 206 (1966).

CHAPTER 2 THE REACTION OF IODINE WITH BIS(DIBUTYLDITHIOCARBAMATO)ZINC(II)

2-1 Introduction

As revealed in Chapter 1, the reaction of bis(diethyldithiocarbamato)dimethyltin(IV) with iodine can best be described in terms of a mechanism involving a charge-transfer complex, formed by an electrophilic attack of I_2 on the sulfur atom of the dithiocarbamato ligand, followed by decomposition in the rate-determining step to afford tetraethylthiuram disulfide, and diethyldithiocarbamatodimethyliodotin(IV) or dimethyldiiodotin(IV). It is of considerable interest to determine whether this mechanism is unique for the tin(IV) complex or whether it represents an example of a more general type of mechanism in the reactions of dithiocarbamato metal complexes with halogens.

This chapter describes the kinetic study on the reaction of bis(dibutyldithiocarbamato)zinc(II), $Zn(n\text{-}Bu_2dtc)_2$, with iodine. This reaction was already reported to give diiodotetrabutylthiuram-disulfidezinc(II), $ZnI_2(n\text{-}Bu_4tds)$, by Brinkhoff, et al.$^{1)}$

2-2 Experimental

Materials. $Zn(n\text{-}Bu_2dtc)_2$ was prepared according to the literature method,$^{2)}$ and recrystallized from ligroin; mp 107°C (ref. 107.3°C). Anal. Found: C, 45.43; H, 7.85; N, 5.88%.

Calcd for $C_{18}H_{36}N_2S_4Zn$: C, 45.60; H, 7.65; N, 5.91%. Iodine and cyclohexane used as the solvent were purified as described in Chapter 1.

Reaction. A solution of I_2 (0.50 mmol) in cyclohexane (20 ml) was added to Zn(n-Bu_2dtc)$_2$ (1.50 mmol) in the same solvent (20 ml) at room temperature. The iodine color disappeared immediately. The solution was stirred for 10 min. The resulting precipitate was filtered and recrystallized from a carbon disulfide/petroleum ether mixture to afford ZnI_2(n-Bu_4tds) (0.45 mmol); mp 152°C. Anal. Found: C, 29.75; H, 5.08; N, 3.93%. Calcd for $C_{18}H_{36}N_2S_4I_2Zn$: C, 29.70; H, 4.99; N, 3.85%.

The stoichiometry of the reaction of I_2 with excess Zn(n-Bu_2dtc)$_2$ is, therefore, expressed as follows;

$$\mathrm{Zn}(n\text{-}\mathrm{Bu_2dtc})_2 + \mathrm{I_2} \longrightarrow \mathrm{ZnI_2}(n\text{-}\mathrm{Bu_4tds}) \qquad (1)$$

Spectra. Electronic spectra were recorded on a Hitachi 124 spectrophotometer. Rapid scanning spectra were measured on a Union RA-1300 stopped-flow rapid scan analyzer.

Kinetics. Kinetic runs were carried out under pseudo-first-order conditions with at least a 20-fold excess amount of Zn(n-Bu_2dtc)$_2$. The reaction rate was followed by measuring the absorbance of the reaction mixture, using a Union RA-102 stopped-flow spectrophotometer equipped with a thermostated cell holder. The temperature was maintained constant to within ±0.1°C.

The decay of absorbance with time was monitored on a Hitachi V-108 memoriscope. Absorbance-time data were obtained by photographing the scope. For each run at least four measurements were carried out. Pseudo-first-order rate constants were obtained from the plots of $\ln(A_t - A_\infty)$ against time, where A_t and A_∞ are absorbances at a given wavelength at a time t and the end of the reaction, respectively. The plots were linear to 80% completion. Rate constants were calculated by the least-squares method.

2-3 Results and Discussion

Rapid scanning spectra of the solution just after mixing of I_2 with excess $Zn(n\text{-}Bu_2dtc)_2$ in cyclohexane are illustrated in Figure 1, which shows a decay of absorbances at 355 and 480 nm both with a half-life of about 50 ms. This result is similar to that obtained in the reaction of dithiocarbamatotin(IV) with I_2 in Chapter 1. Iodine, $Zn(n\text{-}Bu_2dtc)_2$, and $ZnI_2(n\text{-}Bu_4tds)$ do not show any absorption in these regions. The 355 nm band is, therefore, assigned to the charge-transfer transition from the sulfur atom of the dithiocarbamato ligand to I_2 and the 480 nm absorption to the blue-shift band of I_2, as discussed in Ch. 1.

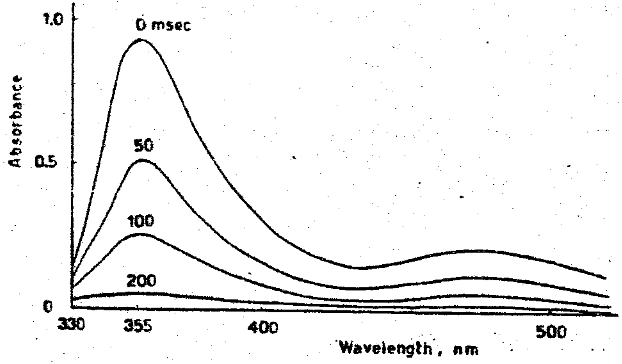

Figure 1. The decay of the electronic spectrum after mixing I_2 (3.00×10^{-4} *M*) with excess $Zn(n\text{-}Bu_2dtc)_2$ (1.00×10^{-2} *M*) in cyclohexane; scanning speed = 150 nm/5 msec, cell length = 1.0 cm.

Thus, the CT complex (1) formed during the period of mixing would be an intermediate in the reaction.

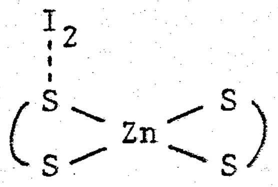

1: S⌒S= $S_2CN(n\text{-}Bu)_2$

The rate of reaction was followed by monitoring the decay of absorbances at 360 and 500 nm. Pseudo-first-order rate constants, k_{obsd}, were evaluated from the slopes of the $\ln(A_t - A_\infty)$ vs. time plots at various concentrations of $Zn(n\text{-}Bu_2dtc)_2$. The results are listed in Table 1.

TABLE I. Observed Rate Constants for the Reaction of I_2 with Excess $Zn(n\text{-}Bu_2dtc)_2$ in Cyclohexane.

Temp (°C)	$10^4[I_2]$ (*M*)	$10^3[Zn(n\text{-}Bu_2dtc)_2]$ (*M*)	k_{obsd} (sec^{-1})	
			360 nm	500 nm
15.0	2.03	6.05	8.53	8.98
		8.02	11.8	11.4
		10.0	16.5	17.3
		12.0	20.9	22.6
		16.0	30.5	32.1
25.0	1.00	2.04	1.63	1.89
		3.01	3.22	3.57
		4.02	4.82	5.21
		5.01	7.73	7.94
		6.00	10.4	10.5
		8.02	15.9	16.1
		10.0	20.6	
		12.0	25.7	
	1.47	3.01	3.04	
		4.50	5.53	
		6.00	8.52	
		7.57	13.8	
		9.00	17.3	
		12.0	23.4	
		15.1	34.6	
	2.02	4.04	4.85	6.12
		8.03	11.6	15.5
		12.0	25.0	25.9
		16.0	35.7	40.5
		20.0	48.7	52.2
35.0	2.03	6.02	10.1	10.8
		8.00	15.5	17.6
		10.0	21.7	24.9
		12.0	27.2	30.6
		16.0	42.6	

The fairly good agreement between the k_{obsd} values at 360 and 500 nm supports the assignment of the absorption bands described above.

The plots of k_{obsd} against the Zn(*n*-Bu_2dtc)$_2$ concentration are shown in Figure 2. There can be seen a linear relationship at high concentrations of Zn(*n*-Bu_2dtc)$_2$. Thus, k_{obsd} is expressed as follows;

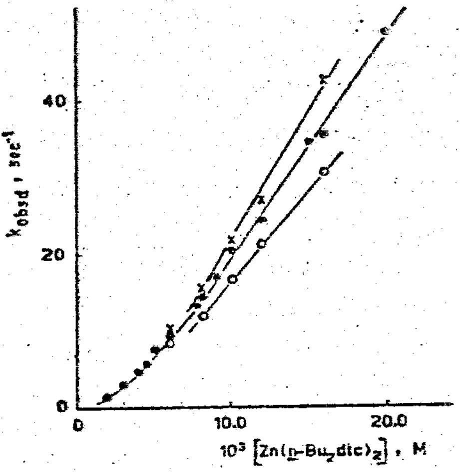

Figure 2. Plots of k_{obsd} (380 nm) against [Zn(n-Bu_2dtc)$_2$]; ○ 15 °C, ● 25 °C, and X 35 °C.

$$k_{obsd} = k[\mathrm{Zn}(n\text{-}\mathrm{Bu_2dtc})_2] \qquad (2)$$

where k is the rate constant of reaction at a fixed concentration of I_2. At lower concentrations of Zn(*n*-Bu_2dtc)$_2$, however, the plots deviate from the straight line. This behavior suggests that the reaction rate may be contributed by higher-order terms of the Zn(*n*-Bu_2dtc)$_2$ concentration. The data were analysed graphically in various manners. As a result, the plots of [Zn(*n*-Bu_2dtc)$_2$]/k_{obsd} against 1/[Zn(*n*-Bu_2dtc)$_2$] gave a straight line over the observed range of excess Zn(*n*-Bu_2dtc)$_2$ concentrations, as depicted in Figure 3. This result suggests the following pathway, (3) and (4).

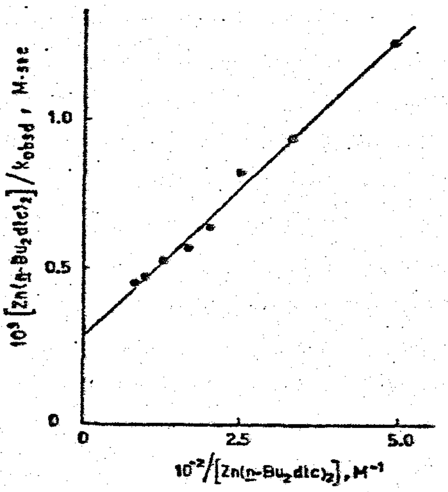

Figure 3. Plots of $[\mathrm{Zn(n\text{-}Bu_2dtc)_2}]/k_{obsd}$ against $1/[\mathrm{Zn(n\text{-}Bu_2dtc)_2}]$ for the reaction of I_2 with excess $\mathrm{Zn(n\text{-}Bu_2dtc)_2}$ at 25 °C; $[I_2] = 1.0 \times 10^{-4}$ M.

$$\mathrm{Zn}(n\text{-}\mathrm{Bu_2dtc})_2 \;+\; \mathrm{I_2} \;\overset{K}{\rightleftharpoons}\; \underset{1}{\mathrm{Zn}(n\text{-}\mathrm{Bu_2dtc})_2\cdot \mathrm{I_2}} \tag{3}$$

$$1 \;+\; \mathrm{Zn}(n\text{-}\mathrm{Bu_2dtc})_2 \;\xrightarrow{k}\; \mathrm{Zn}(n\text{-}\mathrm{Bu_2dtc})_2 \;+\; \mathrm{ZnI_2}(n\text{-}\mathrm{Bu_4tds}) \tag{4}$$

The equation (3) corresponds to the rapid formation of the 1:1 charge-transfer complex of I_2 with $\mathrm{Zn}(n\text{-}\mathrm{Bu_2dtc})_2$, which can react with additional $\mathrm{Zn}(n\text{-}\mathrm{Bu_2dtc})_2$ by a bimolecular manner (Eq. 4).

According to this reaction pathway, k_{obsd} is expressed by Eq. (5). It is evident that the limiting expression (2)

$$k_{obsd} = \frac{Kk[\mathrm{Zn}(n\text{-}\mathrm{Bu_2dtc})_2]^2}{1 + K[\mathrm{Zn}(n\text{-}\mathrm{Bu_2dtc})_2]} \tag{5}$$

at high concentrations of $\mathrm{Zn}(n\text{-}\mathrm{Bu_2dtc})_2$ is readily derived from (5). A transformation of (5) gives (6), which is

$$\frac{[\mathrm{Zn}(n\text{-}\mathrm{Bu_2dtc})_2]}{k_{obsd}} = \frac{1}{Kk}\cdot\frac{1}{[\mathrm{Zn}(n\text{-}\mathrm{Bu_2dtc})_2]} + \frac{1}{k} \tag{6}$$

consistent with the observed rate profile (Figure 3). Thus, K and k were obtained from plots of $[Zn(n\text{-}Bu_2dtc)_2]/k_{obsd}$ against $1/[Zn(n\text{-}Bu_2dtc)_2]$, with intercept 1/k and slope 1/Kk. The results are given in Table 2. The K and k values are independent of the initial concentration of iodine within the experimental error. The K value (1.47×10^2 M^{-1} at 25°C) is compared with those of charge-transfer complexes between I_2 and methyl dimethyldithiocarbamate,3) methyl *N*-methylthiocarbamate,4) or related thiones.3-5)

Table 2 Equilibrium constants and reaction rates for the system of I_2-$Zn(n\text{-}Bu_2dtc)_2$ in cyclohexane.

Temp	$10^4[I_2]$	$10^{-2}K$	$10^{-3}k$
°C	M	M^{-1}	$M^{-1}s^{-1}$
15.0	2.03	2.38 ± 0.18	2.44 ± 0.08
25.0	1.00	1.53 ± 0.27	3.54 ± 0.43
	1.47	1.47 ± 0.12	3.22 ± 0.21
	2.02	1.42 ± 0.13	3.41 ± 0.18
35.0	2.03	1.07 ± 0.13	4.47 ± 0.50

Thermodynamic parameters of the reactions (3) and (4) were determined from K and k at three different temperatures (Table 2). The plot of ln K against 1/T was linear, yielding the values $\Delta H° = -30.2$ kJ/mol and $\Delta S° = -59.4$ J/(molK) for the reaction (3). The Arrhenius plot of ln k against 1/T also gave the values $E_a = 22.9$ kJ/mol and $\Delta S^{\ddagger} = -109$ J/(molK) for the reaction (4). It is to be noted that the activation entropy for the reaction (4) is a large negative value, which is compatible with an associative pathway.

It would be reasonable to assume that the zinc atom of the CT complex (1) is more acidic than that of $Zn(n\text{-}Bu_2dtc)_2$

because of the charge-transfer from the sulfur atom to I_2 in the former. This assumption predicts that the increasing acidity of the zinc atom facilitates the nucleophilic attack of the sulfur atom of the additional $Zn(n\text{-}Bu_2dtc)_2$ molecule to afford a transition state (2), as shown in the Scheme.

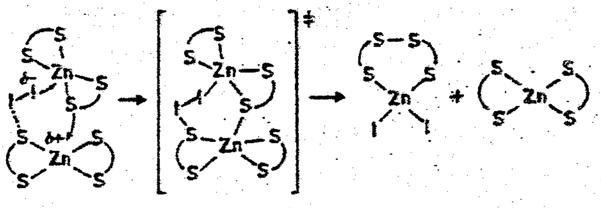

2

The penta-coordination of Zn(II) is well known in solid $Zn(Et_2dtc)_2$ which exists as a dimer (3),6) while it is

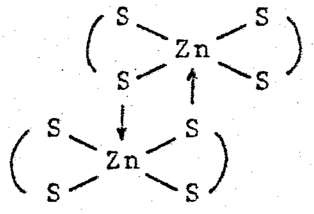

3

monomeric in cyclohexane.7) Although there is no direct evidence for the actual structure of the transition state, an analogous bimolecular mechanism was suggested by Fackler, et al. for the ligand exchange between bis(dithiocumato)zinc(II) and its trithiocumato analog.8)

2-4 Summary

The reaction of bis(dibutyldithiocarbamato)zinc(II), $Zn(n\text{-}Bu_2dtc)_2$, with iodine in cyclohexane was studied employing a stopped-flow technique under pseudo-first-order conditions with excess Zn(n-Bu$_2$dtc)$_2$. The rate data indicate that the reaction proceeds *via* the formation of a charge-transfer complex Zn(n-Bu$_2$dtc)$_2$·I$_2$, and obeys second-order kinetics for the concentration of Zn(n-Bu$_2$dtc)$_2$. These results were interpreted by a mechanism that involves a bimolecular reaction between the charge-transfer complex and the parent Zn(n-Bu$_2$dtc)$_2$ compound. The thermodynamic parameters for the formation of the charge-transfer complex were determined; $K= 1.47 \times 10^2\ M^{-1}$, $\Delta H° = -30.2$ kJ/mol, $\Delta S° = -59.4$ J/(molK) at 25°C. The rate constant and activation parameters for the bimolecular reaction were also determined; $k= 3.43 \times 10^3\ M^{-1}s^{-1}$, $E_a = 22.9$ kJ/mol, $\Delta S^{\ddagger} = -109$ J/(molK) at 25°C, and the transition state of the bimolecular pathway was proposed.

2-5 References

1) H. C. Brinkhoff, J. A. Cras, J. J. Steggerda, and J. Willemse, *Recl. Trav. Chim. Pays-Bas*, 88, 633 (1969).

2) G. D. Thorn and R. A. Ludwig, "The Dithiocarbamates and Related Compounds," Elsevier, Amsterdam, 1962.

3) A. F. Grand and M. Tamres, *Inorg. Chem.*, 8, 2459 (1969).

4) K. R. Bhaskar, S. N. Bhat, A. S. N. Murthy, and C. N. R. Rao, *Trans. Faraday Soc.*, 62, 788 (1966).

5) G. Reichenbach, S. Santini, and U. Mazzucato, *J. Chem. Soc., Faraday Trans. 1*, 69, 143 (1973).

6) M. Bonamico, G. Mazzone, A. Vaciago, and L. Zambonelli, *Acta Cryst.*, 19, 898 (1965).

7) R. E. Morris, *Ind. Eng. Chem.*, 34, 506 (1942).

8) J. P. Fackler, Jr. and J. A. Fetchin, *J. Am. Chem. Soc.*, 92, 2912 (1970).

CHAPTER 3 THE REACTION OF HALOGENS WITH BIS(μ-DIBUTYLDITHIOCARBAMATO-S,S')DIGOLD(I)

3-1 Introduction

Among the two types of reactions of dithiocarbamato metal complexes with halogens; one of them is that the dithiocarbamato ligand is oxidized by halogen to give thiuram disulfide, and the other is the oxidation of the central metal by halogen, as summarized in Table 1 of Chapter 1. Chapters 1 and 2 describe the kinetic study on the former type of reaction. No kinetic study for the latter type of reaction, however, has been reported so far.

This chapter describes the kinetic study on the oxidation reaction of bis(μ-dibutyldithiocarbamato-S,S')-digold(I) by iodine, iodine bromide, and bromine in dichloromethane which belongs to the latter type of reaction. This reaction is known to give bis(dibutyldithiocarbamato)gold(III) dihaloaurate(I).[1, 2]

3-2 Experimental

Materials. Bis(μ-dibutyldithiocarbamato-S,S')-digold(I), [Au(*n*-Bu$_2$dtc)]$_2$, was prepared by the literature method[3] and recrystallized twice from 1,2-dichloroethane. Found: C, 26.70; H, 4.52; N, 3.29%. Calcd for $C_{18}H_{36}N_2S_4Au_2$: C, 26.93; H, 4.52; N, 3.49%.

Iodine and iodine bromide were purified by sublimation and bromine by distillation prior to use. A dichloromethane solution of Br_2 was standardized by 0.01 N $Na_2S_2O_3$ containing 0.1 M KI using starch as an indicator before use. Dichloromethane used as a solvent was purified in the usual method.$^{4)}$

*Reactions of [Au(*n*-Bu$_2$dtc)]$_2$ with Halogens.* A solution of X_2(X_2= I_2, IBr, and Br_2) (0.5 mmol) in CH_2Cl_2(15 ml) was mixed with [Au(*n*-Bu_2dtc)]$_2$(0.5 mmol) in CH_2Cl_2(15 ml) at room temperature to give a dark green (I_2 and IBr) or a red (Br_2) solution, followed by rapid decoloration. The solution was evaporated to dryness under reduced pressure. The resulting solid was recrystallized from acetonitrile to afford yellow needles of $[Au^{III}(n\text{-}Bu_2dtc)_2][Au^{I}X_2]$ (95% based on the amount of gold).

X_2= I_2: mp 135°C (lit.$^{2)}$ 135°C). Found: C, 20.45; H, 3.44; N, 2.57%. Calcd for $C_{18}H_{36}N_2S_4I_2Au_2$: C, 20.46; H, 3.44; N, 2.65%.

X_2= IBr: mp 139°C. Found: C, 21.07; H, 3.49; N, 2.88%. Calcd for $C_{18}H_{36}N_2S_4BrIAu_2$: C, 21.41; H, 3.60; N, 2.78%.

X_2= Br_2: mp 143°C (lit.$^{2)}$ 143-144°C). Found: C, 22.31; H, 3.74; N, 2.91%. Calcd for $C_{18}H_{36}N_2S_4Br_2Au_2$: C, 22.46; H, 3.78; N, 2.91%.

The stoichiometry of reaction of [Au(*n*-Bu_2dtc)]$_2$ with halogens is, therefore, expressed as follows;

$$[Au(n\text{-}Bu_2dtc)]_2 + X_2 \longrightarrow [Au(n\text{-}Bu_2dtc)_2][AuX_2]$$

Spectra. Electronic spectra were recorded on a Hitachi 124 (at 25°C) or a Hitachi 356 (at -50°C) spectrophotometer, the latter of which was equipped with a glass Dewar. Rapid scanning spectra were measured with a Union RA-1300 stopped-flow rapid scan analyzer.

Kinetic Measurements. Kinetic runs were carried out under the conditions where equimolar amounts of the reactants were used and either one of those was used excessively relative to the other. The rate of reaction was followed by monitoring the absorbance at a fixed wavelength in the electronic spectra of the reaction mixture, using a Union RA-413 stopped-flow spectrophotometer equipped with a 0.2 cm quartz cell in a cell holder thermostated within ±0.2°C. Absorbance-time data were accumulated at least five times on a Union System-71 data processor and average absorbance-time curves were recorded using a National VP-6421A X-Y recorder. Plots of $\ln|A_t - A_\infty|$ vs. time were found to be linear to at least 70% completion, where A_t and A_∞ are absorbances at a given wavelength at a time t and the end of the reaction, respectively. Observed first-order rate constants, k_{obsd}, were obtained by performing the least-squares analysis on the linear region of $\ln|A_t - A_\infty|$ vs. time plots.

3-3 Results and Discussion

Rapid Scanning Spectra and a Reaction Intermediate. Figure 1 shows a typical example of rapid scanning spectra for the $[Au(n\text{-}Bu_2dtc)]_2\text{-}I_2$ system. Four absorption peaks at 280, 380, 460, and 630 nm are observed immediately after mixing of the reactants. These bands are weakened with intensifying of the bands newly appeared at 270 and 320 nm, which are assigned to $[Au(n\text{-}Bu_2dtc)_2][AuI_2]$.[2] Then, isosbestic points are found at 275, 305, and 350 nm. This spectral change clearly indicates the occurrence of a transient species as a reaction intermediate.

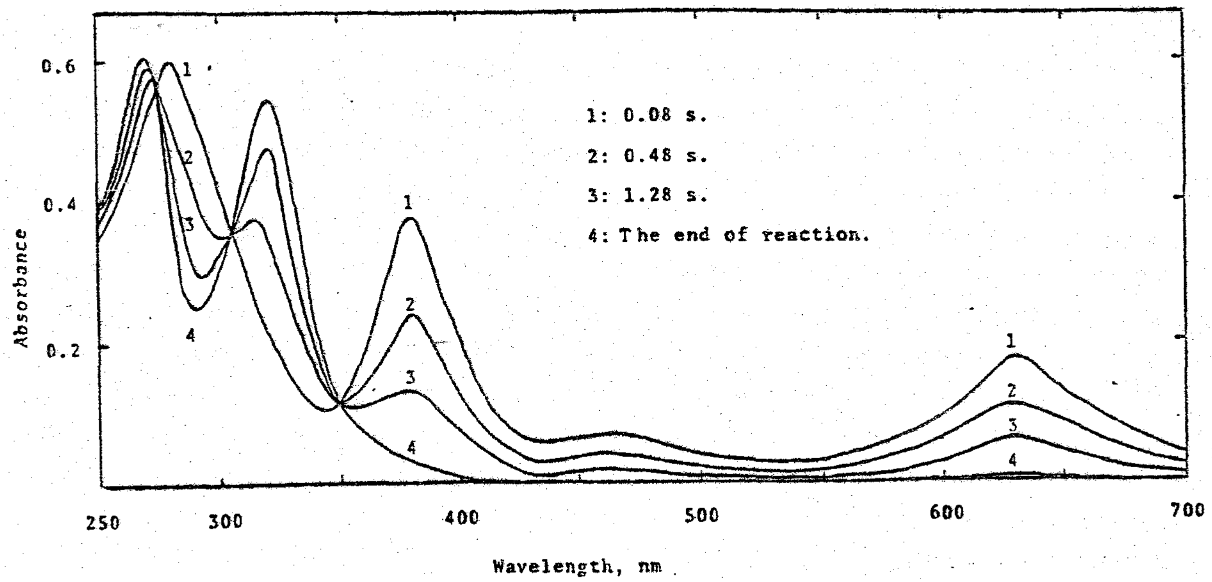

Fig. 1. Rapid scanning spectra of the reaction of $[Au(n\text{-}Bu_2dtc)]_2$ (2.11×10^{-4} M) with I_2 (2.08×10^{-4} M) in CH_2Cl_2 at 25°C; scanning speed= 150 nm/5 ms, cell length= 0.2 cm.

The transient species has been frozen at -50°C; when a dichloromethane solution of $[Au(n\text{-}Bu_2dtc)]_2$ was mixed with iodine in the same solvent at -50°C; the solution immediately displayed green color, which did not disappear over 10 h at this temperature, though a decoloration took place almost instantly above -15°C. The absorption spectrum at -50°C was quite similar to that immediately after mixing at 25°C and the green color can be associated with the 630 nm band. It has been reported that $Au^{II}(Et_2dtc)_2$ exhibits an absorption near 600 nm.5) No esr signal has, however, been detected for the green solution obtained here, indicating that the transient species is not $Au^{II}(n\text{-}Bu_2dtc)_2$. By analogy with kinetic studies of the $Me_2Sn(Et_2dtc)_2\text{-}I_2$ (Chapter 1) and $Zn(n\text{-}Bu_2dtc)_2\text{-}I_2$ (Chapter 2) systems, the 380 nm band can be assigned to the charge-transfer (CT) transition from sulfur of the dithiocarbamato ligand to I_2 and the weak absorption at 460 nm to a blue-shifted band of the iodine moiety of the CT complex. The composition of the CT complex was determined by the mole ratio method in the visible spectrum at -50°C. Figure 2 shows

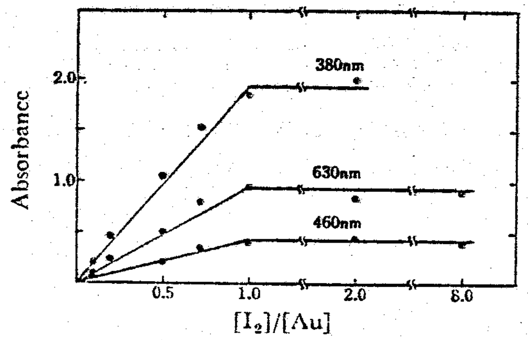

Fig. 2. Mole ratio study of $[Au(n\text{-}Bu_2dtc)]_2$-I_2 system in CH_2Cl_2 at −50 °C; $[[Au(n\text{-}Bu_2dtc)]_2]=5.0\times10^{-5}$ M.

plots of the absorbance at three different wavelengths against the mole ratio of I_2 to the gold(I) complex, indicating the composition of 1:1. It is to be noted that the band characteristic of $[Au(n\text{-}Bu_2dtc)]_2$ underwent only a little shift upon CT complexation (287→280 nm). This fact indicates that the CT complex may retain the parent dimeric structure of $[Au(n\text{-}Bu_2dtc)]_2$. The gold-gold distance in $[Au(n\text{-}Pr_2dtc)]_2$ was reported to be shorter than that in metallic gold,$^{6)}$ however the valence state of Au(I), $5d^{10}$, predicts the presence of no metal-metal bondings. In spite of this, the fact that $[Au(n\text{-}Bu_2dtc)]_2\cdot I_2$ exhibited the absorption band at 630 nm suggests the CT complex involving the skeleton with a gold-gold interaction shown in 1. The Au(I)-Au(I) interaction

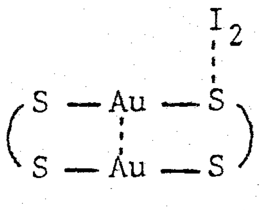

1: S⌒S= $S_2CN(n\text{-}Bu)_2$

would account for the absorption band at 630 nm observed in the CT complex.

The [Au(n-Bu_2dtc)]$_2$-IBr and -Br_2 systems also exhibited absorption maxima due to the CT transition at 380 nm. No blue-shifted band of halogens has, however, been observed in these systems (Table 1). This is probably due to the masking of it by the tail of the intense CT band at 380 nm, because of small molar extinction coefficients of IBr and Br_2 compared with that of I_2; $\varepsilon_{486\ nm} = 3.7 \times 10^2$, $\varepsilon_{406\ nm} = 2.6 \times 10^2$, and $\varepsilon_{505\ nm} = 9.0 \times 10^2\ M^{-1}cm^{-1}$ for IBr, Br_2, and I_2 in CH_2Cl_2, respectively.

Molar extinction coefficients of the absorptions arising from the CT complex were determined from the visible spectra of dichloromethane solutions containing a fixed amount of the Au(I)

Table 1. Electronic spectra of [Au(n-Bu_2dtc)]$_2$, [Au(n-Bu_2dtc)$_2$][AuX_2], and [Au(n-Bu_2dtc)]$_2$·X_2 in CH_2Cl_2 at 25°C.

	λ_{max}	ε		λ_{max}	ε a)
	nm	$M^{-1}cm^{-1}$		nm	$M^{-1}cm^{-1}$
[Au(n-Bu_2dtc)]$_2$	287	4.0×10^4	[Au(n-Bu_2dtc)]$_2$·X_2		
[Au(n-Bu_2dtc)$_2$][AuX_2]			X_2= I_2	280	b)
X_2= I_2	270	4.0×10^4		380	3.9×10^4
	320	3.9×10^4		460	8.3×10^3 c)
IBr	270	3.5×10^4		630	1.8×10^4
	320	3.0×10^4	IBr	280	b)
Br_2	270	3.8×10^4		380	
	320	3.1×10^4		600	
			Br_2	280	
				380	
				560	

a) Calculated from the visible spectrum at -50°C.

b) Not measured.

c) Uncorrected for the contribution from the overlap with the CT band.

complex and large excess I_2 or *vice versa* at -50°C. The result is listed in Table 1 together with the ε values of absorptions due to $[Au(n\text{-}Bu_2dtc)]_2$ and $[Au(n\text{-}Bu_2dtc)_2][AuX_2]$. The ε value of the 380 nm band is very close to those of CT bands of the I_2 complexes with methyl dimethyldithiocarbamate ($\varepsilon_{347\ nm} = 3.0 \times 10^4\ M^{-1}cm^{-1}$) and tetraethylthiuram disulfide ($\varepsilon_{356\ nm} = 3.8 \times 10^4\ M^{-1}cm^{-1}$).7) On the other hand, the value of the blue-shifted band of iodine (460 nm) is larger than those of other known iodine complexes ($\varepsilon_{max} = (2.7\text{-}4.2) \times 10^3\ M^{-1}cm^{-1}$).7-11) This is due to an overlapping of this band with the tail of the CT band.

Kinetics and Mechanism. The rate of reaction was determined by following the decomposition of $[Au(n\text{-}Bu_2dtc)]_2 \cdot X_2$ and the formation of $[Au(n\text{-}Bu_2dtc)_2][AuX_2]$. Observed first-order rate constants, k_{obsd}, obtained from the decay of three band maxima of the CT complex and the rise of a band maximum of the product for the reaction of $[Au(n\text{-}Bu_2dtc)]_2$ with I_2 in CH_2Cl_2 are listed in Table 2, which indicates that the k_{obsd} values obtained from the different wavelengths are consistent with one another within experimental error. They are also essentially the same in various concentrations and varying mole ratios of the reactants, indicating that the reaction is independent of both concentrations of $[Au(n\text{-}Bu_2dtc)]_2$ and I_2 in the measured range. Similar kinetic results were obtained in the $[Au(n\text{-}Bu_2dtc)]_2$-IBr and -Br_2 systems. The k_{obsd} values obtained are listed in Table 3. It is therefore suggested that the reaction of $[Au(n\text{-}Bu_2dtc)]_2$ with halogens proceeds *via* a CT complex, which decomposes to give the final product as follows,

Table 2 Observed rate constants for the reaction of $[Au(n\text{-}Bu_2dtc)]_2$ with I_2 in CH_2Cl_2.

Temp °C	$10^4[I_2]$ M	$10^4[Au]$ M	k_{obsd} s^{-1} 630	460	380	320 nm
25.0	1.04	1.06	2.70		2.04	
	10.4		2.43		2.06	
	20.8		2.60		2.44	
	2.08	2.11	2.51		2.23	2.90
	4.93	5.03	2.65	2.65	2.11	2.87
	39.1		2.46			
	0.946	2.00	2.50		2.68	
		20.0	2.36		2.23	
	1.02	10.0	2.35	2.00	2.05	
		20.4	2.35	2.00	2.17	
		30.3	2.40	2.28	2.38	
		39.6	2.06	2.14	2.29	
		49.8	2.39	2.25	2.10	
15.5	1.01	9.80	1.15	1.35	1.13	
		20.0	1.21	1.27	1.11	
		29.9	1.27	1.21	1.17	
		40.0	1.26	1.10	1.14	
		50.0	1.25	1.51	1.30	
20.2	0.62	30.2	1.70	1.80	1.83	
	1.23		1.69		1.82	
	2.46		1.74	1.79	1.86	
	4.93		1.81	1.68	1.80	
	1.02	10.0	1.68	1.66	1.66	
		20.4	1.83	1.63	1.76	
		30.3	1.58	1.72	1.69	
		39.3	1.83	1.77	1.76	
		49.8	1.83	1.73	1.86	
	1.50	15.2	1.60	1.53	1.58	
		20.0	1.94	1.78	1.74	
		40.0		1.94	1.89	
10.1	1.02	20.4	1.07	1.02	1.04	
	2.05		0.925	0.929	0.842	
	4.10		0.812	0.710	0.834	
	1.02	10.2	0.892	0.850	0.880	
	2.05		0.854	0.780	0.840	

Table 3 Observed rate constants for the reaction of $[Au(n\text{-}Bu_2dtc)]_2$ with IBr or Br_2 in CH_2Cl_2.

Temp	10^4[IBr]	10^4[Au]	k_{obsd}		Temp	$10^4[Br_2]$	10^4[Au]	k_{obsd}	
°C	M	M	s^{-1}		°C	M	M	s^{-1}	
			600	380 nm				560	380 nm
24.8	2.00	20.0	1.13	1.11	25.4	3.09	13.4	1.21	1.36
	10.0	10.0	1.22	1.02			26.8		1.30
		20.0	1.15	1.06			53.6	1.24	1.23
	20.0		1.29	1.05		1.29	10.0	1.26	1.45
	100		1.21	1.29		5.00	21.1	1.42	1.28
20.8	67.7	20.0	1.04		20.2	1.91	14.4	1.22	1.37
	33.9		1.18	1.18			28.8	1.27	1.15
	13.9		1.01	0.990			43.5	1.25	1.16
15.3	0.986	20.0	1.08	0.902			57.6	1.22	1.27
	9.86		0.709	0.659	15.4	1.18	12.5	1.09	1.11
	19.7		0.617	0.539			25.0	1.10	1.14
	98.6		0.715	0.951			38.5	1.12	1.14
	9.86	10.1	0.774	0.620			50.0	1.11	1.05
	19.7		1.17	1.15	10.5	2.06	15.1	0.927	1.16
11.1	2.00	20.0	0.869	0.820			30.1	0.879	0.950
	20.0		0.595	0.562			45.0	0.950	0.846
	100		0.540	0.527			60.3	1.02	1.03
	10.0		0.777	0.737					

$$\begin{tikzcd}[\mathrm{Au}(n\text{-}\mathrm{Bu_2dtc})]_2 + \mathrm{X_2} \arrow[r, "\text{fast}"] & [\mathrm{Au}(n\text{-}\mathrm{Bu_2dtc})]_2\cdot \mathrm{X_2} \arrow[d, "k"] \\ & [\mathrm{Au}(n\text{-}\mathrm{Bu_2dtc})_2][\mathrm{AuX_2}]\end{tikzcd}$$

where k is equal to k_{obsd}. According to this scheme, the rate law can be written as,

$$\frac{d[[\mathrm{Au}(n\text{-}\mathrm{Bu_2dtc})_2][\mathrm{AuX_2}]]}{dt} = -\frac{d[[\mathrm{Au}(n\text{-}\mathrm{Bu_2dtc})]_2\cdot \mathrm{X_2}]}{dt}$$

$$= k[[\mathrm{Au}(n\text{-}\mathrm{Bu_2dtc})]_2\cdot \mathrm{X_2}].$$

Rate constants and activation parameters obtained from the Eyring plots of ln(k/T) against 1/T are summarized in Table 4.

Table 4 Rate constants and activation parameters for the reaction of $[\mathrm{Au(n\text{-}Bu_2dtc)}]_2$ with X_2 in CH_2Cl_2.a)

X_2	Temp °C	k s^{-1}	$\Delta H^{\ddagger}_{298}$ $kJmol^{-1}$	$\Delta S^{\ddagger}_{298}$ $Jmol^{-1}K^{-1}$
I_2	10.1	0.89 ± 0.09	43.7 ± 8.4	-91.5 ± 28.9
	15.5	1.23 ± 0.10		
	20.2	1.75 ± 0.10		
	25.0	2.35 ± 0.24		
IBr	11.1	0.68 ± 0.13	26.0 ± 16.1	-156 ± 55
	15.3	0.82 ± 0.21		
	20.8	1.08 ± 0.08		
	24.8	1.15 ± 0.09		
Br_2	10.5	0.97 ± 0.09	12.3 ± 5.6	-201 ± 19
	15.4	1.11 ± 0.03		
	20.2	1.24 ± 0.07		
	25.4	1.31 ± 0.08		

a) Errors quoted are standard deviations.

Although there is no direct evidence for another transient species, at least two possible intermediates, 2 and 3, can be envisaged in the decomposition pathway.

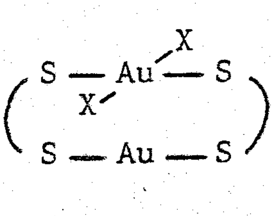
2

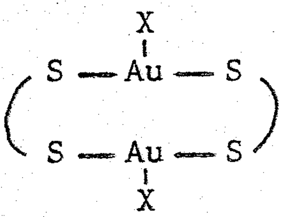
3

Intermediate 2 which is a mixed valence gold(III)-gold(I) complex may be formed by the attack of iodine at a single gold atom. Alternatively, the simultaneous attack of iodine at both gold atoms will afford the gold(II) complex, 3. The existence of both 2 and 3 may be supported from the fact that analogous gold complexes, 4 and 5, were isolated in the oxidation reactions of

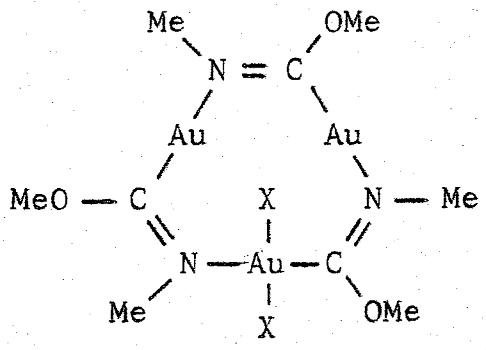
4

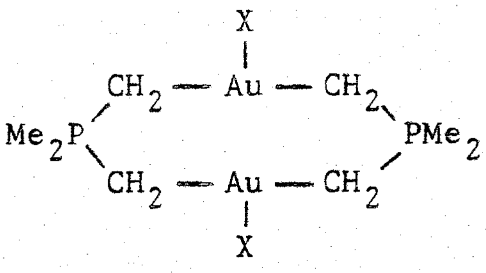
5

trimeric$^{12)}$ and dimeric$^{13)}$ gold(I) complexes with halogen, respectively. Of the two possible intermediates, however, 2 is more appealing since it requires a less reorganization of atoms, followed by reductive elimination at the gold(III) center to afford the final product, [Au(n-Bu$_2$dtc)$_2$][AuX$_2$].

3-4 Summary

Kinetics of the reaction of bis(μ-dibutyldithiocarbamato-S,S')-digold(I), [Au(*n*-Bu_2dtc)$]_2$, with I_2, IBr, and Br_2 in dichloromethane was studied by a stopped-flow technique. A 1:1 charge-transfer complex, [Au(*n*-Bu_2dtc)$]_2 \cdot X_2$ (X_2= I_2, IBr, and Br_2), formed in the initial process of reaction was identified spectrophotometrically at -50°C. The rates of reaction were almost the same for I_2, IBr, and Br_2, and independent of the both [Au(*n*-Bu_2dtc)$]_2$ and halogen concentrations. The reaction was interpreted to proceed *via* the charge-transfer complex, [Au(*n*-Bu_2dtc)$]_2 \cdot X_2$, which decomposes in a rate-determining step to give the final product, [Au(*n*-Bu_2dtc$)_2$][AuX_2]. The activation parameters for the reactions were determined: $\Delta H^{\ddagger}$(kJ/mol)= 43.7 (I_2), 26.0 (IBr),and 12.3 (Br_2); $\Delta S^{\ddagger}$(J/(mol K)) = -91.5 (I_2), -156 (IBr), and -201 (Br_2).

3-5 References

1) H. J. A. Blaauw, R. J. F. Nivard, and G. J. M. van der Kerk, *J. Organomet. Chem.*, 2, 236 (1964).

2) P. T. Beurskens, H. J. A. Blaauw, J. A. Cras, and J. J. Steggerda, *Inorg. Chem.*, 7, 805 (1968).

3) S. Akerstrom, *Arkiv Kemi*, 14, 387 (1959).

4) J. A. Riddick and E. E. Toops, Jr., "Technique of Organic Chemistry," Vol. 7, 2nd ed., ed. by A. Weissberger, Interscience, New York, N. Y. (1955), p. 409.

5) S. Akerstrom, *Arkiv Kemi*, 14, 403 (1959); and T. Vangard and S. Akerstrom, *Nature*, 184, 183 (1959).

6) R. Hesse and P. Jennische, *Acta Chem. Scand.*, 26, 3855 (1972).

7) A. F. Grand and M. Tamres, *Inorg. Chem.*, 8, 2459 (1969).

8) R. P. Lang, *J. Am. Chem. Soc.*, 84, 1185 (1962).

9) K. R. Bhaskar, S. N. Bhat, A. S. N. Murthy, and C. N. R. Rao, *Trans. Faraday Soc.*, 62, 788 (1966).

10) G. Reichenbach, S. Santini, and U. Mazzucato, *J. Chem. Soc., Faraday Trans.1*, 69, 143 (1973).

11) M. Tamres, "Molecular Complexes," Vol. 1, ed. by R. Foster, Paul Elek Ltd, London (1973), p. 98.

12) A. L. Balch and D. J. Doonan, *J. Organomet. Chem.*, 131, (1977).

13) H. Schmidbaur and R. Franke, *Inorg. Chim. Acta*, 13, 85 (1975); and H. Schmidbaur, J. R. Mandl, A. Frank, and G. Huttner, *Chem. Ber.*, 109, 466 (1976).

CHAPTER 4 THE REACTION OF THE DITHIOCARBAMATES OF COPPER(I) AND SILVER(I) WITH THIURAM DISULFIDE

4-1 Introduction

In previous chapters, the oxidation reactions of dithiocarbamate complexes of tin(IV), zinc(II), and gold(I) with halogens are discussed, where the reactions can best be described in terms of a mechanism involving a charge-transfer complex formed by electrophilic attack of halogen on the sulfur atom of the dithiocarbamate ligand. As an extension of these works, the present chapter reports kinetic and mechanistic studies on the oxidation reactions of copper(I) and silver(I) complexes of dithiocarbamate by thiuram disulfide, giving bis(dithiocarbamato)copper(II) and silver(II).

4-2 Experimental

Materials. (Dialkyldithiocarbamato)copper(I), $[Cu(R_2dtc)]_4$ (R= Et and *n*-Pr),[1] (dialkyldithiocarbamato)silver(I), $[Ag(R_2dtc)]_6$ (R= Et, *n*-Pr, and *i*-Pr),[2] and tetraalkylthiuram disulfide, R_4tds (R= Et, *n*-Pr, and *i*-Pr),[2] were prepared according to the literature methods. Analytical data for these complexes (C, H, N) were satisfactory. Dichloromethane used as a solvent was purified as described in Chapter 3.

Spectra and Kinetics. Electronic spectra were recorded on a Hitachi 124 spectrophotometer. Rapid scanning spectra were measured with a Union RA-413 stopped-flow rapid scanning spectrophotometer equipped with a 0.2 cm quartz cell in a cell holder thermostated within ±0.2°C. The rate of reaction was followed by monitoring the absorbance at a fixed wavelength in the electronic spectra of the reaction mixture under pseudo-first-order conditions, using at least a ten-fold excess of thiuram disulfide. Absorbance-time data were accumulated at least five times on a Union System-71 data processor and average absorbance-time curves were recorded using a National VP-6421A X-Y recorder. Pseudo-first-order rate constants, k_{obsd}, were calculated from the slope of a linear part of the $\ln(A_\infty - A_t)$ vs. time plots by the least-squares method, where A_∞ and A_t are absorbances at the end of the reaction and at a time t, respectively.

4-3 Results and Discussion

Reaction of $[Cu(R_2dtc)]_4$ with R_4tds. The reaction of $[Cu(R_2dtc)]_4$ with R_4tds rapidly proceeds to give bis(dialkyldithiocarbamato)copper(II), $Cu(R_2dtc)_2$, in quantitative yields.[3)] The stoichiometry of reaction can, therefore, be expressed as Eq. (1). A typical rapid scanning spectrum after mixing the

$$\frac{1}{4}[Cu(R_2dtc)]_4 + \frac{1}{2}R_4tds \longrightarrow Cu(R_2dtc)_2 \qquad (1)$$

reactant solutions is shown in Figure 1. An absorption band at 303 nm observed immediately after mixing is identical in wavenumber with that of the reactant $[Cu(Et_2dtc)]_4$ (λ_{max} = 303 nm, ε_{max} = 4.5×10^4 $M^{-1}cm^{-1}$ in CH_2Cl_2). The final spectrum

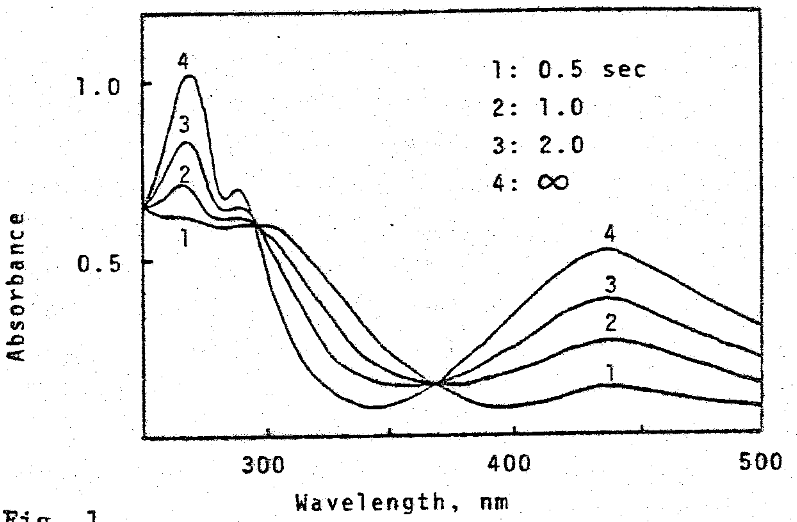

Fig. 1
Spectral changes after mixing of $[Cu(Et_2dtc)]_4$ (5.1×10^{-5} M) with Et_4tds(1.0×10^{-4} M) in CH_2Cl_2 at 25°C.

with three absorption peaks at 270, 290, and 435 nm is assigned to $Cu(Et_2dtc)_2$ ($\varepsilon = 3.1 \times 10^4$, 1.8×10^4, 1.2×10^4 $M^{-1}cm^{-1}$ in CH_2Cl_2, respectively).[3-6] Half-lives of these absorption bands were almost identical with one another, and isosbestic points are found at 295 and 370 nm.

The rate data of reaction (1) (R= Et and *n*-Pr) were obtained from increase of the absorbance at 435 nm. Figure 2 shows a

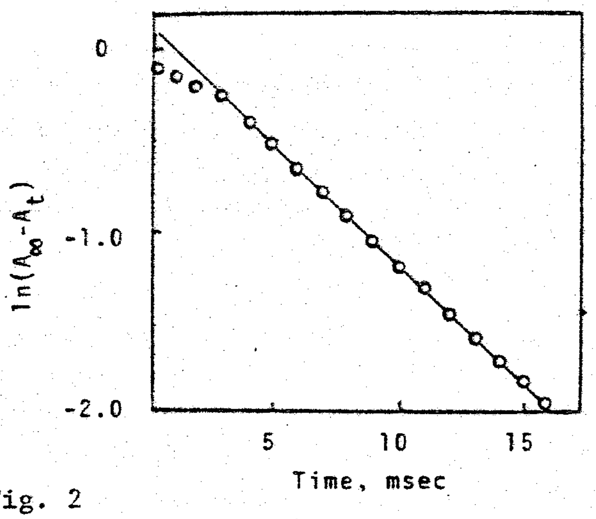

Fig. 2
Plots of $\ln(A_\infty - A_t)$ against time at 25°C; $[[Cu(Et_2dtc)]_4] = 1.0 \times 10^{-4}$ M, $[Et_4tds] = 1.0 \times 10^{-2}$ M.

typical example of $\ln(A_\infty - A_t)$ vs. time plots. Except for initial several milliseconds, a good linear relation between them is obtained for at least 80% completion of the reaction. The linear part of plots was used to determine the value of pseudo-first-order rate constants. Table 1 lists the rate data at various concentrations of $[Cu(R_2dtc)]_4$ and R_4tds. All the plots of k_{obsd} vs. the concentration of R_4tds at each temperature yielded straight lines with zero intercepts. This result may suggest the following pathways.

$$[Cu(R_2dtc)]_4 \overset{+R_4tds}{\rightleftarrows} [Cu(R_2dtc)\cdot R_4tds] + [Cu(R_2dtc)]_3 \overset{+R_4tds}{\rightleftarrows} \cdots \qquad K_{o}, \quad (2)$$

$$[Cu(R_2dtc)\cdot R_4tds] \longrightarrow Cu(R_2dtc)_2 + R_2dtc\cdot \qquad k \quad (3)$$

$$2\ R_2dtc\cdot \xrightarrow{\text{fast}} R_4tds \qquad (4)$$

Equation (2) consists of multi-step equilibrium reactions, where tetrameric compound $[Cu(R_2dtc)]_4$ dissociates by an attack of R_4tds to form an adduct, $[Cu(R_2dtc)\cdot R_4tds]$, and the trimer $[Cu(R_2dtc)]_3$, the latter of which successively reacts with R_4tds to form the adduct in a similar manner. The initial curvature of $\ln(A_\infty - A_t)$ vs. time plots (Figure 2) may correspond to a preequilibrium immediately after mixing, where the concentration of the adduct does not reach a steady state. Although there is no direct evidence for the formation of the adduct as an intermediate, several metal complexes of thiuram disulfide have been isolated,7-9) and the dissociation of $[Cu(Et_2dtc)]_4$ by the attack of Et_2dtc^- (Eq. 5) has been reported.1)

$$[Cu^{I}(Et_2dtc)]_4 + 4\ Et_2dtc^- \longrightarrow 4\ [Cu^{I}(Et_2dtc)_2]^- \qquad (5)$$

Table 1 Pseudo-first-order rate constants for the reaction of $[Cu(R_2dtc)]_4$ with R_4tds in CH_2Cl_2.

R	Temp	10^4[Cu]	10^4[tds]	k_{obsd}
	°C	M	M	s^{-1}
Et	10.5	0.501	20.0	12.8
			40.0	28.0
			59.7	44.3
			80.9	59.3
			100	73.5
	12.5	1.00	100	82.8
			200	156
			301	264
			400	314
			500	413
	15.5	0.501	20.0	18.4
			40.0	33.6
			59.7	48.8
			80.9	70.4
			100	89.0
	16.9	1.00	100	100
			200	214
			301	317
			400	450
			500	523
	20.1	0.501	20.0	24.9
			40.0	43.9
			59.7	65.4
			80.9	83.1
Et	20.1	1.00	100	115
			200	243
			301	312
			400	481
	25.0	0.505	10.0	14.3
		1.51	20.1	18.8
		0.625	25.0	38.2
		0.505	40.0	52.3
			50.1	66.3
			80.0	93.4
		1.00	100	127
			200	245
			301	349
n-Pr	10.9	0.529	20.8	6.37
			40.0	13.6
			60.4	21.3
			79.7	28.2
			99.8	35.3
	15.8	0.529	20.8	7.31
			40.0	17.3
			60.4	23.7
			79.7	32.1
			99.8	42.3
n-Pr	20.3	0.513	20.1	11.5
			40.0	23.0
			50.1	29.1
			61.5	36.8
		0.529	60.4	31.6
			79.7	39.7
			100	50.4
		1.08	100	51.9
			203	94.4
			302	151
			401	195
			500	221
	25.0	1.28	20.1	14.7
		0.513	39.8	25.5
		1.28		28.7
		0.513	50.1	33.1
		1.28		37.0
		0.513	61.5	44.3
		1.28		42.3
		0.513	79.7	53.7
			100	65.5
		1.08	100	63.4
		0.513	123	74.7
		1.08	203	134
			302	192
			401	244
			500	276

Thus, two possible structures, 1 and 2, are proposed for the adduct between the copper(I) complex and thiuram disulfide.

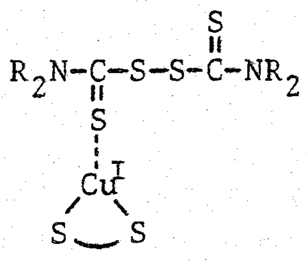

1: $S\frown S = S_2CNR_2$

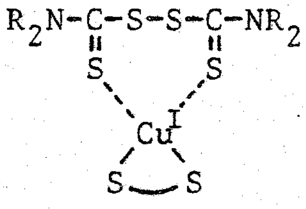

2

In either case the adduct may be decomposed in a rate-determining step (Eq. 3), which involves cleavage of the S-S bond of thiuram disulfide to give the oxidized copper(II) product, $Cu(R_2dtc)_2$, and the $R_2dtc\cdot$ radical. The resulting radical may rapidly dimerize to afford the thiuram disulfide as reported by Dauquis and Lechenal,$^{10)}$ who have estimated the rate constant to be $2 \times 10^5\ M^{-1}s^{-1}$ in CH_3CN.

According to the pathway of (2)-(4), the k_{obsd} value in the presence of excess thiuram disulfide is expressed by Eq. (6),

$$k_{obsd} = \frac{K_\circ k[R_4tds]}{1 + K_\circ[R_4tds]} \qquad (6)$$

where $K_\circ$ stands for the multi-step equilibrium constant in Eq. (2). If one assumes $K_\circ[R_4tds] \ll 1$, Eq. (6) can be reduced to Eq. (7), which predicts a linear relationship between k_{obsd}

$$k_{obsd} = K_\circ k[R_4tds] \qquad (7)$$

and $[R_4tds]$ with the slope of $K_\circ k$ and zero intercept. This is consistent with the observed rate profile. Table 2 lists the value of $K_\circ k$ and activation parameters determined from the

Table 2 Kinetic and activation parameters for the reaction of $[Cu(R_2dtc)]_4$ with R_4tds in CH_2Cl_2.[a)]

R	Temp °C	$10^{-3}K_\circ k$ $M^{-1}s^{-1}$	$\Delta H^{\ddagger}$ $kJmol^{-1}$	$\Delta S^{\ddagger}$ $Jmol^{-1}K^{-1}$
Et	25.0	11.7 ± 0.2	20.6 ± 4.4	-97 ± 10
	20.1	11.7 ± 0.5		
	16.9	10.8 ± 0.5		
	15.5	8.86 ± 0.35		
	12.5	8.19 ± 0.44		
	10.5	7.60 ± 0.11		
n-Pr	25.0	5.70 ± 0.09	18.2 ± 3.1	-112 ± 10
	20.3	4.52 ± 0.10		
	15.8	4.29 ± 0.19		
	10.9	3.67 ± 0.03		

a) Errors quoted are standard deviations.

Arrhenius plot of $\ln(K_\circ k)$ vs. 1/T.

Reaction of $[Ag(R_2dtc)]_6$ *with* R_4*tds.* The addition of R_4tds to a dichloromethane solution of $[Ag(R_2dtc)]_6$ immediately causes a blue color, which becomes more intense as more R_4tds is added. Although the blue $Ag(R_2dtc)_2$ complex has not been isolated, its presence in solution was confirmed on the basis of the appearance of an absorption maximum at ~600 nm in the electronic spectrum.[3, 6)] Stoichiometry for the reaction of $[Ag(R_2dtc)]_6$ with R_4tds (R= Et, *n*-Pr, and *i*-Pr) is expressed as Eq. (8), and the equilibrium constants (K) in $CHCl_3$ at 20°C

$$\frac{1}{6}\,[Ag(R_2dtc)]_6 \;+\; \frac{1}{2}\,R_4tds \;\underset{}{\overset{K}{\rightleftharpoons}}\; Ag(R_2dtc)_2 \qquad (8)$$

(see Table 3) were determined spectrophotometrically by

Table 3 Equilibrium constants and thermodynamic parameters for the reaction of $[Ag(R_2dtc)]_6$ with R_4tds in CH_2Cl_2.a)

R	Temp °C	K M^{-1}	ΔH° $kJmol^{-1}$	ΔS° $Jmol^{-1}K^{-1}$
Et	25.8	$(4.46 \pm 0.23)x10^{-4}$	23.0 ± 1.0	12.9 ± 7.4
	20.5	$(3.80 \pm 0.22)x10^{-4}$		
		$(3.8x10^{-4})$ b)		
	15.1	$(3.14 \pm 0.24)x10^{-4}$		
	10.0	$(2.71 \pm 0.27)x10^{-4}$		
n-Pr	24.7	$(4.85 \pm 0.32)x10^{-4}$	27.9 ± 0.4	30.2 ± 3.1
	20.4	$(4.16 \pm 0.34)x10^{-4}$		
		$(5.5x10^{-4})$ b)		
	15.5	$(3.51 \pm 0.29)x10^{-4}$		
	9.7	$(2.66 \pm 0.34)x10^{-4}$		
i-Pr	24.5	$(9.21 \pm 0.13)x10^{-3}$	16.4 ± 0.4	16.2 ± 3.3
	20.6	$(8.43 \pm 0.34)x10^{-3}$		
		$(1.1x10^{-2})$ b)		
	15.3	$(7.35 \pm 0.35)x10^{-3}$		
	11.0	$(6.65 \pm 0.26)x10^{-3}$		

a) Errors quoted are standard deviations.

b) In $CHCl_3$ at 20°C; ref 3.

Akerstrom.3) We also determined the K value in CH_2Cl_2 at four different temperatures by the spectrophotometric method (Table 3). Plots of ln(K) vs. 1/T gave linear relations, from which thermodynamic parameters of the reaction (8) were obtained. The results are listed in Table 3, which shows the equilibrium lies so far to the left. The fact that the K value when R= *i*-Pr is larger than those when R= *n*-Pr and Et may be due to a large inductive effect of the isopropyl group than the *n*-propyl and ethyl groups of the dithiocarbamate ligand, resulting in increasing stability of $Ag(R_2dtc)_2$ by delocalization of the electronic charge as shown in b of the canonical structures in general introduction.

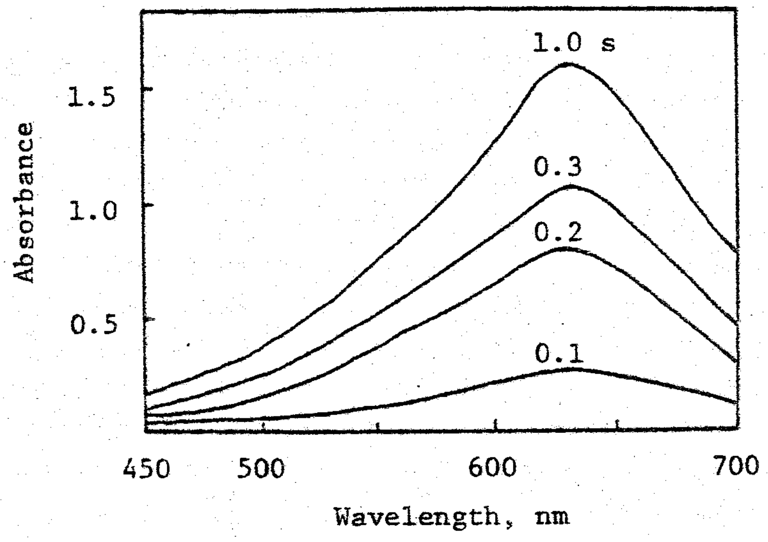

Fig. 3 Spectral changes after mixing of $[Ag(i\text{-}Pr_2dtc)]_6$(5.0×10^{-4} M) with $i\text{-}Pr_4tds$(5.0×10^{-2} M) in CH_2Cl_2 at 25°C.

A typical change of electronic spectra in the visible region after mixing of the reactants is depicted in Figure 3, which clearly shows the formation of $Ag(i\text{-}Pr_2dtc)_2$ (λ_{max}= 620 nm, ε_{max}= 1.3×10^4 $M^{-1}cm^{-1}$ in CH_2Cl_2; lit.[3] λ_{max}= 620 nm in $CHCl_3$). There was seen little change in the ultraviolet spectra, because the equilibrium of Eq. (8) lies so far to the left. The rate of reaction was, therefore, followed by measuring the absorbance at 620 nm (R= *i*-Pr) or 600 nm (R= Et and *n*-Pr). Plots of $\ln(A_\infty - A_t)$ vs. time were found to be linear to at least 80% completion except for the initial short period after mixing, as was seen in the copper complexes (Figure 2). Pseudo-first-order rate constants obtained from a linear region of the plots are listed in Table 4. Plots of k_{obsd} vs. the concentration of R_4tds showed pronounced curvature at high concentrations of R_4tds. A typical example is shown in Figure 4, which is in contrast

Table 4 Pseudo-first-order rate constants for the reaction of $[Ag(R_2dtc)]_6$ with R_4tds in CH_2Cl_2.

R	Temp	10^4[Ag]	10^4[tds]	k_{obsd}	R	Temp	10^4[Ag]	10^4[tds]	k_{obsd}	R	Temp	10^4[Ag]	10^4[tds]	k_{obsd}
	°C	M	M	s^{-1}		°C	M	M	s^{-1}		°C	M	M	s^{-1}
Et	10.6	5.02	100	0.108	n-Pr	10.3	5.00	100	0.0993	i-Pr	10.2	4.99	100	0.762
			200	0.187				200	0.136				201	1.01
			300	0.221				299	0.164				301	1.17
			400	0.262				400	0.205				400	1.32
			500	0.270				500	0.235				501	1.40
	15.2	5.02	100	0.179		15.2	5.00	100	0.163		14.9	4.99	100	1.15
			200	0.271				200	0.261				201	1.55
			300	0.357				299	0.315				301	1.84
			400	0.421				400	0.321				400	2.01
			500	0.468				500	0.360				501	2.22
	20.3	5.02	100	0.302		20.0	5.00	100	0.289		20.0	5.00	100	1.91
			200	0.456				200	0.414				201	2.55
			300	0.562				299	0.482				301	2.92
			400	0.669				400	0.585				400	3.13
			500	0.724				500	0.670				501	3.36
	25.0	5.02	200	0.788		25.1	5.00	100	0.503		25.1	5.00	100	3.03
			300	0.980			10.0		0.501				201	4.12
			400	1.13			5.00	200	0.673				301	4.68
			500	1.30			10.0		0.786				400	5.05
							5.00	300	0.942				501	5.54
							10.0		0.828					
							5.00	400	1.04					
							10.0		0.952					
							5.00	500	1.04					
							10.0		1.11					

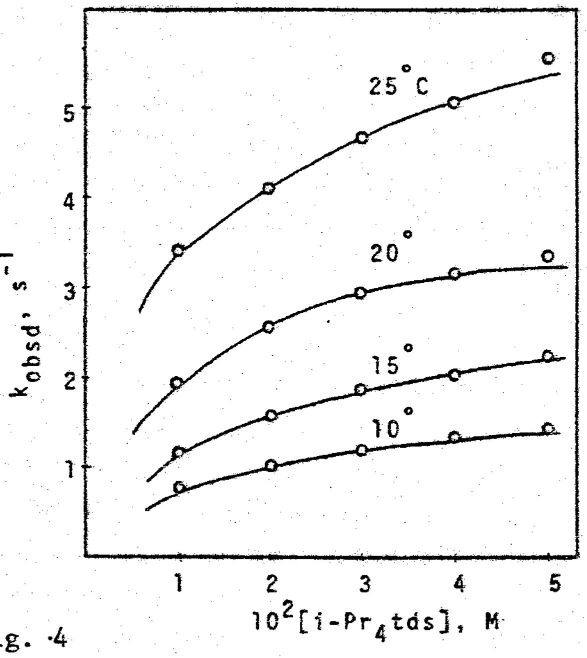

Fig. 4

Plots of k_{obsd} against [i-Pr_4tds]; $[[Ag(i\text{-}Pr_2dtc)]_6] = 5.0 \times 10^{-4}$M.

to the linear relationship for the copper system. This characteristic difference can be explained by the assumption that the multi-step equilibrium constant K₀ is larger in the silver system than in the copper one.

The mechanism proposed above for the copper system is, therefore, applicable to this reaction. The reaction pathways can be postulated as Eqs. (9) and (10), followed by dimerization

$$[Ag(R_2dtc)]_6 \underset{}{\overset{+R_4tds}{\rightleftarrows}} [Ag(R_2dtc)\cdot R_4tds] + [Ag(R_2dtc)]_5 \overset{+R_4tds}{\rightleftarrows} \cdots \qquad K_\circ, \quad (9)$$

$$[Ag(R_2dtc)\cdot R_4tds] \longrightarrow Ag(R_2dtc)_2 + R_2dtc\cdot \qquad k, \quad (10)$$

of the $R_2dtc\cdot$ radical according to Eq. (4). Moreover, the divalent silver complex, $Ag(R_2dtc)_2$, formed by Eq. (10) is expected to degrade because of its instability at or around room temperature. Similar instability has been reported for bis(diethylmonothiocarbamato)copper(II) complex,11) which rapidly undergoes rearrangement to a hexameric monovalent copper complex according to Eq. (11). By analogy with this,

$$Cu(SOCNEt_2)_2 \longrightarrow \frac{1}{6}\,[Cu(SOCNEt_2)]_6 + \frac{1}{2}\,(Et_2NC(O)S)_2 \qquad (11)$$

$Ag(R_2dtc)_2$ is possible to undergo transformation as shown in Eq. (12). Thus, Eqs. (9), (10), (4), and (12) constitute a

$$Ag(R_2dtc)_2 \longrightarrow \frac{1}{6}\,[Ag(R_2dtc)]_6 + \frac{1}{2}\,R_4tds \qquad k', \quad (12)$$

cyclic equilibrium for the $[Ag(R_2dtc)]_6$-R_4tds system. According to this system, the equilibrium constant, K, for the overall reaction (Eq. 8) is equal to $K_\circ k/k'$. If $k \ll k'$, then k_{obsd} is also given by Eq. (6) in the presence of excess R_4tds. It is apparent from Eq. (6) that the plots of k_{obsd} vs. $[R_4tds]$ show a curvature at so high concentrations of R_4tds as $K_\circ[R_4tds]$ is ~1. This is consistent with the observed kinetics (Figure 4). Eq. (6) can be transformed to Eq. (13), which predicts that

$$\frac{1}{k_{obsd}} = \frac{1}{K_\circ k[R_4tds]} + \frac{1}{k} \qquad (13)$$

there should be a linear relationship between $1/k_{obsd}$ vs. $1/[R_4tds]$, with the intercept of $1/k$ and the slope of $1/K_\circ k$. An example of the plots is depicted in Figure 5, which shows a linear relation over the observed range of R_4tds concentrations The rate and equilibrium constants for the $[Ag(R_2dtc)]_6$-R_4tds system are summarized in Table 5. It should be noted that the k' values (Eq. 12) are the same order of magnitude as the rate constant of dimerization of the $R_2dtc\cdot$ radical in CH_3CN (2×10^5 $M^{-1}s^{-1}$).[10] In view of this result, the reaction of $Ag(R_2dtc)_2$ with $R_2dtc\cdot$ (Eq. 14) may be in competition with that of Eq. (12).

Table 5 Equilibrium and rate constants for the reaction of $[Ag(R_2dtc)]_6$ with R_4tds in CH_2Cl_2.a)

R	Temp °C	K_o M^{-1}	k s^{-1}	k' b) s^{-1}
Et	25.0	28.2 ± 4.2	2.17 ± 0.30	(1.37 ± 0.29) x 10^5
	20.3	38.4 ± 3.9	1.08 ± 0.10	(1.09 ± 0.16) x 10^5
	15.2	31.8 ± 5.0	0.74 ± 0.11	(7.45 ± 1.71) x 10^4
	10.6	30.4 ± 4.7	0.47 ± 0.07	(5.27 ± 1.25) x 10^4
n-Pr	25.1	49.1 ±12.3	1.50 ± 0.34	(1.52 ± 0.52) x 10^5
	20.0	48.8 ± 9.0	0.87 ± 0.15	(1.02 ± 0.27) x 10^5
	15.2	45.6 ± 6.5	0.53 ± 0.68	(6.83 ± 8.95) x 10^4
	10.3	47.9 ±11.6	0.30 ± 0.07	(5.38 ± 1.97) x 10^4
i-Pr	25.1	86.7 ± 5.3	6.57 ± 0.31	(6.18 ± 0.49) x 10^4
	20.0	89.4 ± 4.6	4.03 ± 0.16	(4.27 ± 0.32) x 10^4
	14.9	71.2 ± 6.5	2.73 ± 0.21	(2.64 ± 0.34) x 10^4
	10.2	79.6 ± 8.3	1.70 ± 0.13	(2.03 ± 0.27) x 10^4

a) Errors quoted are standard deviations.

b) Calculated using $k' = K_o k/K$.

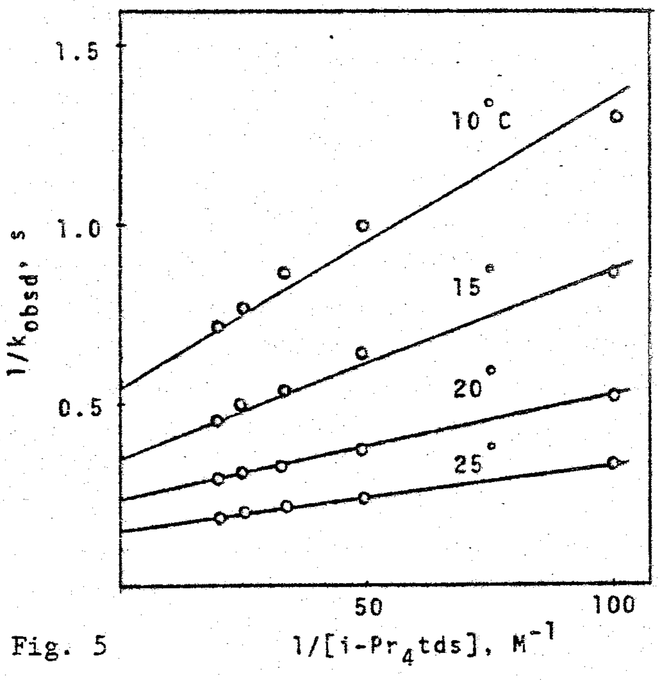

Fig. 5

Plots of $1/k_{obsd}$ against $1/[i\text{-}Pr_4tds]$; $[[Ag(i\text{-}Pr_2dtc)]_6] = 5.0 \times 10^{-4}$M.

$$\mathrm{Ag(R_2dtc)_2} + \mathrm{R_2dtc\cdot} \longrightarrow \frac{1}{6}\,[\mathrm{Ag(R_2dtc)}]_6 + \mathrm{R_4tds} \qquad k', \quad (14)$$

The rate constant of transformation of $Ag(R_2dtc)_2$ into $[Ag(R_2dtc)]_6$ (k' in Eqs. 12 and/or 14) is larger in R= Et and *n*-Pr than in R= *i*-Pr, whereas the rate constant of formation of $Ag(R_2dtc)_2$ (k in Eq. 10) is in an opposite tendency. These are related with the fact that the K value of Eq. (8) is larger with R= *i*-Pr than with R= *n*-Pr and Et, as mentioned above.

Thermodynamic and activation parameters calculated from $K_\circ$, k, and k' at four different temperatures (Table 5) are summarized in Table 6, which reveals that the $\Delta H^\circ_{K_\circ}$ values are near zero. The $\Delta S^\circ_{K_\circ}$ term is, therefore, a dominant factor to cause the reaction (9). The positive $\Delta S^\circ_{K_\circ}$ values are consistent with the stepwise dissociation of $[Ag(R_2dtc)]_6$ by the attack of R_4tds. The small negative $\Delta S^\ddagger_k$ values suggest that the reaction (10) undergoes a small structural change in the transition state. A transition state such as 3 or 4 is, therefore, proposed, where making of the Ag-S bond between the monovalent silver and the disulfide sulfur is somewhat advanced over the S-S bond breaking

Table 6 Thermodynamic and activation parameters for the reaction of $[Ag(R_2dtc)]_6$ with R_4tds in CH_2Cl_2 at 25°C.[a)]

R	$\Delta H^\circ_{K_\circ}$	$\Delta S^\circ_{K_\circ}$	$\Delta H^\ddagger_k$	$\Delta S^\ddagger_k$	$\Delta H^\ddagger_{k'}$	$\Delta S^\ddagger_{k'}$
	$kJmol^{-1}$	$Jmol^{-1}K^{-1}$	$kJmol^{-1}$	$Jmol^{-1}K^{-1}$	$kJmol^{-1}$	$Jmol^{-1}K^{-1}$
Et	-1 ± 7	29 ± 50	70.1 ± 4.1	-4 ±28	42.5 ± 2.5	-3.82 ± 0.14
n-Pr	2 ± 1	38 ± 10	74.1 ± 0.8	-2 ± 5	46.3 ± 3.1	8.98 ± 0.39
i-Pr	6 ± 4	59 ± 29	59.0 ± 1.1	-32 ± 8	50.5 ± 3.2	15.8 ± 0.7

a) Errors quoted are standard deviations.

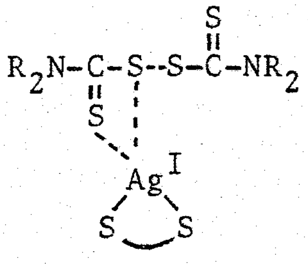

3

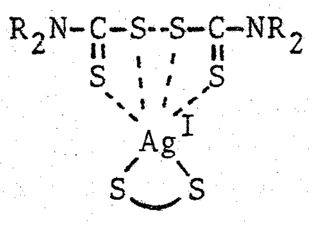

4

of thiuram disulfide.

Finally, it should be mentioned that the $K_o k$ values for the copper system are about two orders greater than those for the silver system in similar experimental conditions (Table 2 and 5). In addition, the finding of a linear dependence of k_{obsd} on the concentration of thiuram disulfide for the copper system predicts that the K_o value is not so large as that for the silver system, as described above. Thus, the k values for the copper system must be more than 2 orders greater than those for the silver system. This is in agreement with the fact that the oxidation to a bivalent state is easier in Cu(I) complexes than in Ag(I) complexes.12)

4-4 Summary

Kinetics of the oxidations of dithiocarbamato-copper(I) and -silver(I) complexes, $[M(R_2dtc)]_n$ (M= Cu, n=4, R= Et, *n*-Pr; M= Ag, n= 6, R= Et, *n*-Pr, *i*-Pr), with the corresponding tetraalkylthiuram disulfide, R_4tds, were investigated in dichloromethane employing a stopped-flow technique. The rate law in the presence of excess R_4tds is expressed as $v = K_o k[R_4tds][[M(R_2dtc)]_n]/(1 + K_o[R_4tds])$, where $K_o k(25°C) = 1.17 \times 10^4$ (Et), 5.70 x 10^3 (*n*-Pr) $M^{-1}s^{-1}$ with $K_\circ \ll 100$ for the copper system, and $K_\circ$(at 25°C)= 28.2(Et), 49.1(*n*-Pr), 86.7(*i*-Pr) M^{-1} and k (25°C)= 2.17(Et), 1.50(*n*-Pr), 6.57(*i*-Pr) s^{-1} for the silver system. The reaction has been interpreted to proceed by a mechanism involving a rapid equilibration (*1*) (the multi-step

$$[M(R_2dtc)]_n \overset{+R_4tds}{\rightleftharpoons} [M(R_2dtc)\cdot R_4tds]+[M(R_2dtc)]_{n-1} \overset{+R_4tds}{\rightleftharpoons} \cdots \qquad (1)$$

equilibrium constant= $K_\circ$) to form an adduct, $[M(R_2dtc)\cdot R_4tds]$, which is decomposed in a rate-determining step (the rate constant= k) yielding the final product, $M(R_2dtc)_2$. The activation parameters were also determined and the nature of the transition state was discussed.

4-5 References

1) A. R. Hendrickson, R. L. Martin, and N. M. Rohde, *Inorg. Chem.*, 15, 2115 (1976).

2) S. Akerstrom, *Arkiv Kemi*, 14, 387 (1959).

3) S. Akerstrom, *Arkiv Kemi*, 14, 403 (1959).

4) P. Petterson and T. Vangard, *Arkiv Kemi*, 17, 249 (1961).

5) T. R. Reddy and R. Srinivasan, *J. Chem. Phys.*, 43, 1404 (1965).

6) M. V. Rajasekharan, C. N. Sethulakshmi, P. T. Manaharan, and H. Gudel, *Inorg. Chem.*, 15, 2657 (1976).

7) H. C. Brinkhoff, J. A. Cras, J. J. Steggerda, and J. Willemse, *Recl. Trav. Chim. Pays-Bas*, 88, 633 (1969).

8) G. Contreras and H. Cortes, *Inorg. Nucl. Chem. Lett.*, 6, 225 (1970).

9) R. M. Golding and W. C. Tennant, *Mol. Phys.*, 24, 301 (1972); R. A. Palmer, W. C. Tennant, M. F. Dix, and A. D. Rae, *J. Chem. Soc., Dalton Trans.*, 1976, 2345.

10) G. Dauquis and D. Lechenal, *J. Electroanal. Chem. Interfacial Electrochem.*, 43, 205 (1973).

11) S. Akerstrom, *Arkiv Kemi*, 24, 479 (1965).

12) F. A. Cotton and G. Wilkinson, "Advanced Inorganic Chemistry, 3rd ed., Interscience, New York, N. Y. (1972), p. 905 and 1044.

CONCLUSION

This study was undertaken to elucidate the mechanism of oxidation reactions of dithiocarbamato metal complexes with halogens and thiuram disulfide. The results of the present work are summarized as follows.

(1) The reactions of dithiocarbamato tin(IV) complexes, $Me_2Sn\text{-}L(S_2CNEt_2)$ (L= S_2CNEt_2 and I) with iodine in cyclohexane were investigated employing a stopped-flow technique. The kinetic data indicate that the reaction in the presence of a large excess of $Me_2SnL(S_2CNEt_2)$ proceeds *via* a charge-transfer complex of $Me_2SnL(S_2CNEt_2)\cdot I_2$, which decomposes in the rate-determining step to yield $Me_2SnI(L)$ and unstable $[I(S_2CNEt_2)]$. This unstable intermediate reacts with the excess $Me_2SnL(S_2CNEt_2)$ to afford $Me_2SnI(L)$ and tetraethylthiuram disulfide. The reaction of $Me_2Sn(S_2CNEt_2)_2$ with a large excess of I_2 was also kinetically studied to reveal the formation of the 1:2 complex, $Me_2Sn(S_2CNEt_2)_2\cdot 2I_2$, as an intermediate, which undergoes a simultaneous degradation to afford Me_2SnI_2 and tetraethylthiuram disulfide. The transition state in the reaction was discussed.

(2) The reaction of bis(dibutyldithiocarbamato)zinc(II), $Zn(S_2CN(n\text{-}Bu)_2)_2$, with iodine in cyclohexane was studied employing a stopped-flow technique under pseudo-first-order conditions with excess $Zn(S_2CN(n\text{-}Bu_2)_2)_2$. The rate data indicate that the reaction proceeds *via* the formation of of a charge-transfer complex $Zn(S_2CN(n\text{-}Bu)_2)_2\cdot I_2$, and obeys second-order kinetics on the concentration of $Zn(S_2CN(n\text{-}Bu)_2)_2$.

These results are interpreted by a mechanism that involves a bimolecular reaction between the charge-transfer complex and the parent $Zn(S_2CN(n\text{-}Bu)_2)_2$ compound. The thermodynamic parameters for the formation of the charge-transfer complex were determined, and the transition state in the bimolecular pathway was proposed.

(3) Kinetics of the reaction of bis(μ-dibutyldithiocarbamato-S,S')-digold(I), $[Au(S_2CN(n\text{-}Bu)_2)]_2$, with I_2, IBr, and Br_2 in dichloromethane was studied by a stopped-flow technique. A 1:1 charge-transfer complex, $[Au(S_2CN(n\text{-}Bu)_2)]_2 \cdot X_2$ (X_2= I_2, IBr, and Br_2), formed in the initial process of reaction was identified spectrophotometrically at -50°C. The rates of reaction were almost the same for I_2, IBr, and Br_2, and independent of the both $[Au(S_2CN(n\text{-}Bu)_2)]_2$ and halogen concentrations. The reaction has been interpreted to proceeds *via* the charge-transfer complex, which decomposes in a rate-determining step to give the final product, $[Au(S_2CN(n\text{-}Bu)_2)_2]$-$[AuX_2]$. The activation parameters for the reactions were determined.

(4) Kinetics of the oxidation of dithiocarbamato-copper(I) and -silver(I) complexes, $[M(S_2CNR_2)]_n$ (M= Cu, n= 4, R= Et, *n*-Pr; M= Ag, n= 6, R= Et, *n*-Pr, *i*-Pr), with the corresponding tetraalkylthiuram disulfide, $(R_2NC(S)S\}_2$, were investigated in dichloromethane employing a stopped-flow technique. The reaction has been interpreted to proceed by a mechanism involving a rapid equilibration to form an adduct, $[M(S_2CNR_2) \cdot (R_2NC(S)S\}_2]$, which is decomposed in a rate-determining step yielding the final product, $M(S_2CNR_2)_2$.